Fission-Track Analysis: Field Collection, Sample Preparation and Data Acquisition

2

Barry Kohn, Ling Chung and Andrew Gleadow

Abstract

Fission-track (FT) analysis for geological applications involves a range of practical considerations, which are reviewed here. These include field sampling, the separation of the most commonly used minerals (apatite, zircon and titanite), the preparation of these minerals for analysis (including for double or triple-dating of the same grains) and measurement of the essential parameters required. Two main analytical strategies are described, the External Detector Method (EDM) and Laser Ablation-Inductively Coupled Plasma-Mass Spectrometry (LA-ICP-MS). Although the initial steps ranging from sample selection to mineral separation are common to both approaches, the next practical steps vary with the specific dating strategy adopted. The workflow outlined here for sample preparation and aspects of data acquisition follows a widely used standard sequence of steps, but some of the specific details described are those developed over many years by the Melbourne Thermochronology Group. While these protocols may be readily applicable or adaptable, it is recognised that many laboratories may have developed their own particular recipes for different aspects of these methods.

2.1 Introduction

This chapter focuses on the practical details of FT analysis for geological applications. Several works have been published emphasising other aspects of FT thermochronology including the fundamental principles, interpretation of data, statistics and application to geological problems; these include Fleischer et al. (1975), Wagner and van den Haute (1992), Gallagher et al. (1998), Dumitru (2000), Gleadow et al. (2002), Tagami and O'Sullivan (2005), Donelick et al. (2005), Kohn et al. (2005), Galbraith (2005), Braun et al. (2006) and Lisker et al. (2009). The topics covered here include field sampling and identification of suitable target material, step-by-step mineral separation and sample preparation (including double- or triple-dating of the same grains), and measurement of the key parameters required for FT thermochronology. Some of the methods outlined for sample preparation and aspects of data acquisition are commonly used and follow a sequence of steps, while the Melbourne Thermochronology Group has specifically developed some others over many years. These protocols are regarded as being readily applicable, if required, to most laboratories carrying out routine FT analysis at this time. However, we emphasise that the methods described here are in no way meant to be prescriptive and it is acknowledged that other laboratories will often have developed their own procedures for certain aspects of sample preparation and data acquisition. In general, proper training conducted by the laboratory supervisor involving an induction process covering relevant procedures and familiarity with Occupational, Health and Safety (OH & S) requirements (especially for handling strong chemicals, heavy liquids and radioactive material) should be an essential first-step for all users who wish to work in a FT laboratory.

2.2 FT Dating Strategies

For FT dating, the most common strategy for studying minerals is the External Detector Method (EDM), which involves sending off polished grain mounts for a thermal neutron irradiation in a nuclear reactor (see Chap. 1, Hurford 2018). More recently however, Laser Ablation-Inductively Coupled Plasma-Mass Spectrometry (LA-ICP-MS) has emerged as an alternative method for the direct acquisition of uranium content in target minerals (Hasebe et al. 2004). Only these two techniques will be

B. Kohn (✉) · L. Chung · A. Gleadow
School of Earth Sciences University of Melbourne, Melbourne, VIC 3010, Australia
e-mail: b.kohn@unimelb.edu.au

M. G. Malusà and P. G. Fitzgerald (eds.), *Fission-Track Thermochronology and its Application to Geology*, Springer Textbooks in Earth Sciences, Geography and Environment, https://doi.org/10.1007/978-3-319-89421-8_2

considered here, as they remain the best alternatives in most FT dating situations. Fundamental age equations for age calculation related to using these methods have been reviewed by Wagner and van den Haute (1992), Gleadow et al. (2002), Hasebe et al. (2004), Tagami and O'Sullivan (2005) and Donelick et al. (2005) (see Chap. 1, Hurford 2018 and Chap. 6, Vermeesch 2018).

In FT dating by EDM, alternative strategies are possible for measuring the ratio of spontaneous (ρ_s) to induced (ρ_i) track densities, upon which the age depends. Not all of these dating strategies are equally reliable in every case, and care is required to ensure that an appropriate method is selected. In practice, a variety of factors such as the registration geometry of the etched surface, accumulated radiation damage, anisotropic etching and uneven intra-grain uranium distribution must be considered when selecting a suitable method of FT dating for a particular sample. The various FT dating methods differ importantly in the registration geometries of the etched surfaces used to count spontaneous and induced tracks, and the corrections required if these are not equivalent. All of these methods, however, require first that the uranium-bearing mineral grains sought be physically separated from their host rock as outlined in Sect. 2.4 and Fig. 2.1. However, the next practical steps after that may rely on the specific dating strategy adopted.

Previous reports describing different laboratory procedures for FT analysis in some detail include Naeser (1976), Hurford and Green (1982), Gleadow (1984), Wagner and van den Haute (1992), Ravenhurst and Donelick (1992), Dumitru (2000), Gleadow et al. (2002), Donelick et al. (2005), Tagami (2005) and Bernet and Garver (2005). Here, we briefly review some of the main steps required for FT analysis, emphasising some recently developed procedures that have become available over the past decade or so.

For volcanic glass, relatively homogeneous uranium concentrations occur between fragments (shards) or within bulk samples (e.g. obsidian). The separation steps, mounting and etching conditions for volcanic glass are outlined in Sects. 2.4–2.6. In most types of natural glass, fission tracks are not fully stable at ambient temperatures over geological time, therefore different methods are used for age determination than the two mentioned above. These will not be discussed further here, but for more information see Dumitru (2000 and references therein) and for a more recent glass dating protocol using a less complicated age correction procedure in combination with a LA-ICP-MS procedure (i.e. no neutron irradiation required) see Ito and Hasebe (2011).

2.3 Sample Collection—Suitable Geological Materials

2.3.1 Sample Collection

Where possible the freshest and cleanest rock material available should be collected for analysis. It is advantageous to remove as much biological material, soil and weathered surface (the outer few centimetres) as possible and break down samples into fist-sized pieces, while sampling *in the field*. Fire prone areas should be avoided if possible, as heat may affect the ability of some minerals to retain their daughter products. However, if sampling is carried out in such areas, then at least the outer ~3 cm of a bedrock sample should be removed (e.g. Reiners et al. 2007). If importing samples from overseas, then the steps outlined above will help to alleviate any concerns by local Quarantine and Customs Authorities.

Wear safety glasses whenever hammering rocks. For some highly altered lithologies, you may have to use a percussion hammer to obtain fresh material. Ensure that samples are *representative* of the lithology being examined and that all are in situ from outcrops. For detrital samples, especially recent or loosely consolidated sediment, it may be possible to do some 'gold panning' in the field in order to obtain a first-order heavy mineral separation and reduce the sample size (e.g. Bernet and Garver 2005). It is critical when sampling to accurately record (usually with a GPS) the sample location, i.e. horizontal datums (in latitude and longitude or another coordinate system) and vertical datums (as either elevation or depth). This is particularly important for future 'users' of the data and for databases.

Depending on the rock type, outcrop samples generally ranging in weight from ~1–3 kg should be collected, but larger samples (~4–7 kg) are recommended from loose sediments, which haven't been panned in the field (e.g. Bernet and Garver 2005). Some samples, such as from cores or cuttings in drill holes, will invariably be much smaller than 1 kg. If drill hole samples are very small, it might be possible to combine samples from a range of limited depths, i.e. over a few 10's m, to form a single sample. For drill hole cuttings, it is important to ensure that down-hole cavings or contamination (particularly from drilling mud) are not a problem. For dating of tephra, near-source coarser pumice blocks or pumiceous lapilli are less likely to be contaminated, but when working with pumiceous material it is critical to ensure that potential contaminants in vesicles have been removed by ultrasonic cleaning. For more distal,

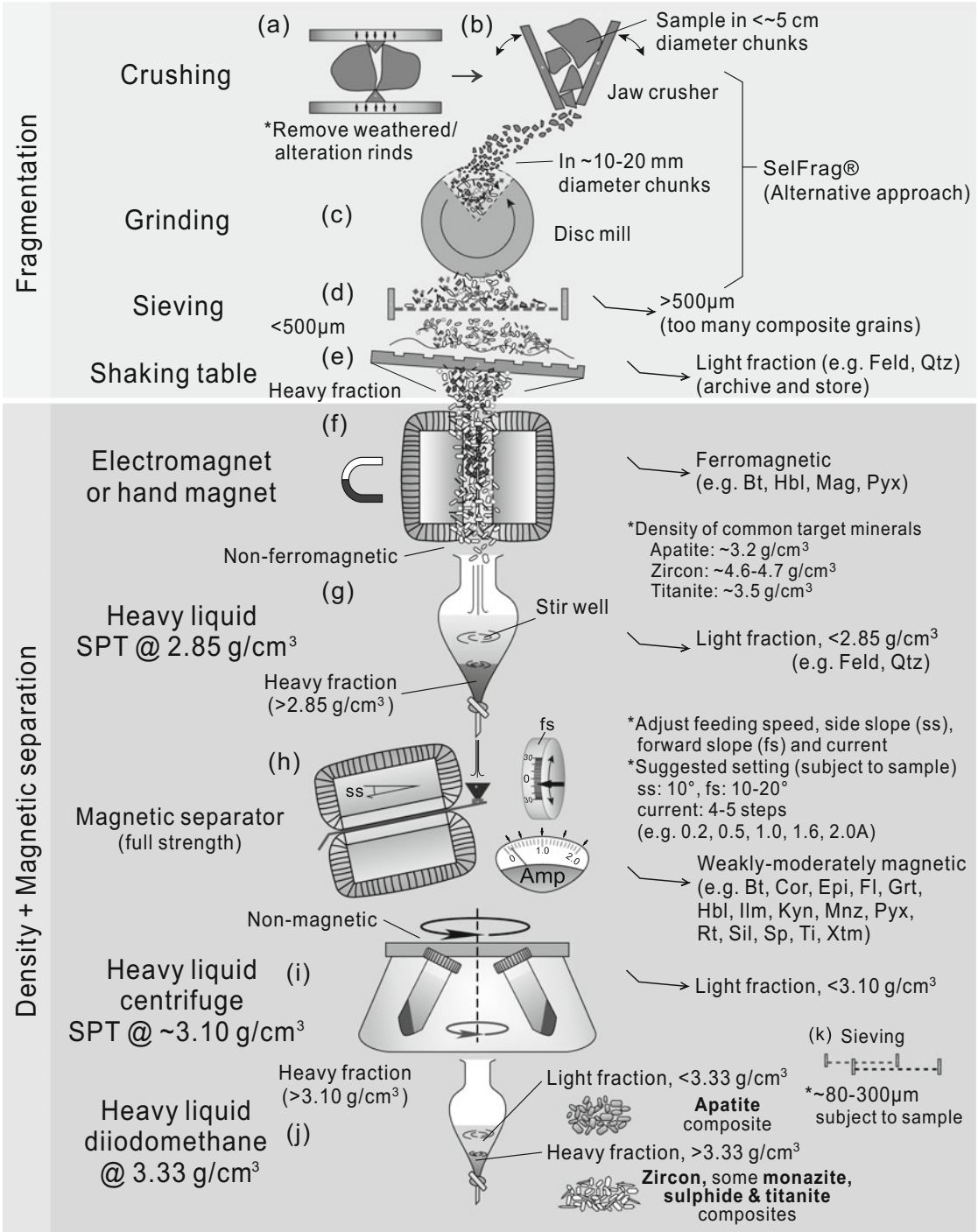

Fig. 2.1 Flow chart showing generalised sequence of steps and conditions for the separation of minerals suitable for FT analysis. See text for further details

Table 2.1 General lithology guide for target minerals sought for FT analysis

Preferred	Less favourable to problematic
• Igneous rocks: silicic to intermediate intrusives (granite, granodiorite, diorite, tonalite) and volcanics (lavas and pyroclastics) and less commonly basic intrusives (gabbro) • Metamorphic rocks: gneisses, granulites, amphibolites, meta-sandstones, some schists • Sedimentary rocks: immature sandstones, red beds, arkoses, some conglomerates and greywackes, occasionally more mature sandstones and quartzites	• Mafic volcanic rocks • Ultramafic rocks • Eclogites • Mafic schists (often contain metamorphic titanite and apatite, but with low U content) • Shales, slates and phyllites • Siltstones and claystones • Mylonites • Evaporites and carbonates (although see dating of detrital minerals in carbonates by Arne et al. 1989) • Highly altered or mineralised rocks (but see Gleadow and Lovering 1974 for mineral suitability in strongly weathered rocks)

thinner and finer tephra, it is important to sample from as deep as possible within the outcrop and to search for the coarsest material available, at the same time taking every precaution to ensure that there has been no potential contamination from overlying beds. Common lithologies containing minerals routinely used for FT thermochronology are summarised in Table 2.1.

2.3.2 Suitable Minerals

Etching studies have revealed fission tracks in more than 100 uranium-bearing minerals and glasses (e.g. Fleischer et al. 1975; Wagner and van den Haute 1992). But factors such as uranium content, track stability characteristics and mineral abundance result in very few of these minerals being routinely analysed for FT thermochronology. The most widely dated minerals are apatite, zircon and titanite. These are commonly present as primary accessory minerals in many igneous and metamorphic rocks and as detrital components in some sedimentary rocks (see Table 2.1). The annealing behaviour of other minerals, which could potentially be used in FT studies, most notably epidote group minerals and some types of garnets and micas are not well understood and their uranium content may be quite low and variable, thus they are not generally suitable for rigorous study. Volcanic, pseudotachylitic, impact and man-made glasses have also been dated occasionally (see Wagner and van den Haute 1992, their Chap. 6.2.11).

2.4 Mineral Separation

Mineral separations for FT dating aim at recovering relatively clean concentrates of suitable uranium-bearing accessory minerals. This is achieved by rock fragmentation, crushing and use of a shaking table (if available) followed by the exploitation of differences in mineral density using heavy liquids and differences in magnetic susceptibility. The steps described here and summarised in Fig. 2.1 are a general, widely used sequence. While many have been tried and tested, it is recognised that some laboratories may use different specific procedures during the workflow (e.g. Donelick et al. 2005; see also Chap. 7, Malusà and Garzanti 2018).

Many of the finer points are not easy to describe, thus there is no substitute for the actual hands-on acquisition of these skills in a functioning laboratory. It is emphasised that absolute cleanliness at each stage of rock crushing and mineral separation is of paramount importance. The final data obtained are only as good as the attention given to prevent possible contamination by foreign mineral grains.

2.4.1 Rock Fragmentation

Prior to commencing rock fragmentation, remove any remaining weathered rind or surfaces possibly exposed to fire (within ~3 cm of the outer surface) with a diamond saw, wire brush or rock splitter. If possible, it is most advantageous if these outer layers are removed and samples broken down into fist-sized pieces, while sampling in the field. Hard rock samples must first be reduced into small pieces using either a hammer or a mechanical splitter, followed by processing through a jaw crusher to produce smaller rock fragments. A wide variety of crushing and grinding equipment can be used to further reduce the particle size and disaggregate grains; this will often be a disc pulveriser with a rotating plate grinding mill fitted with hardened steel plates. In this case, it is crucial to properly adjust the mill plates to minimise the yield of mineral composites (mostly in fractions >500 μm), but at the same time prevent over-grinding of grains, which may result in grains being too small and unsuitable for FT analysis. Once the particle size for a sample has been adequately reduced, samples should be sieved to yield a fraction <500 μm, which may then be passed over a shaking table (e.g. Wilfley or Gemini) if available. This procedure can greatly speed up the separation

process, allowing large samples (several kilograms) to be processed and a heavy mineral fraction concentrated. However, if samples are fine-grained or very small, it is best to avoid using a shaking table and in the case of the former, they should be thoroughly washed with tap water to decant off the finer material (e.g. Donelick et al. 2005). A general scheme is summarised in Fig. 2.1a–e. The separation process is then continued with the heavy concentrate, which first needs to be dried either by heating at low temperature (~50 °C) or rinsing in acetone.

SelFrag® An alternative approach to the mechanical fragmentation of rocks and liberation of minerals as described above, but which requires considerable capital investment in equipment and infrastructure, is through an electrodynamic disaggregation method. This protocol seeks to break grains along their boundaries or internal grain discontinuities. In recent years, this possibility has been achieved through the development of the selFrag Lab®. Studies on apatite and zircon grains, which were liberated using this protocol, have been compared with samples separated by conventional mechanical preparation as described above and indicate no adverse affects for FT thermochronology (Giese et al. 2009; Sperner et al. 2014).

2.4.2 Gravity Separation Using Heavy Liquids and Magnetic Separation

As most target minerals are usually of higher density (>3.2 g/cm^3) and non- or weakly magnetic, combined heavy liquid and magnetic (using a Frantz® Isodynamic Magnetic Separator) separation allows for refinement of the mineral concentrate and removal of any minerals of lighter density not required. Figure 2.1f–j summarises a commonly used sequence of steps for heavy liquid and magnetic separation, although these can vary with sample grain size and mineral composition. Repeated heavy liquid and magnetic separation (using settings with varying degrees of magnetic susceptibility) (see Fig. 2.1h) may provide further purification.

In the past, many laboratories used heavy liquids that are volatile and classed as toxic chemicals such as bromoform (specific gravity 2.89 g/cm^3) and tetrabromoethane (TBE) (specific gravity ~2.96 g/cm^3). However, these have now been largely replaced by non-toxic lithium metatungstate (LMT), lithium heteropolytungstate (LST, density ~2.9 g/cm^3 at 25 °C) and sodium polytungstate (SPT) (Callahan 1987; Torresan 1987; Chisholm et al. 2014), as well as diiodomethane (DIM), also known as methylene iodide (density ~3.31 g/cm^3 at 25 °C).

Two additional methodologies previously reporting the effective use of liquids for carrying out mineral separations are:

- Use of organic liquids for diluting heavy liquids (bromoform and DIM) to create a range of liquid densities, which maintain relatively constant specific gravities for use and storage, as well as an efficient method for recovery of heavy liquids (Ijlst 1973).
- Froth flotation of crushed and sieved sand-size mineral fractions employs chemicals that change the electrical surface properties of specific minerals and make them selectively hydrophobic. When air is blown into a suspension, hydrophobic grains stick to ascending air bubbles and concentrate in a foam on the surface of the flotation cell. Hejl (1998) outlined the practical steps for what is described as a low cost procedure for the successful separation of apatite and zircon from silicate rocks.

For magnetic separation—make sure the Frantz and operating environment is absolutely clean. Use compressed air on the feed hopper, chute and collection buckets and wipe with alcohol. Set the Frantz with a forward slope of 10°–20° (depending on sample) and a side-slope (top towards back) of +10°. These settings can be varied somewhat for special applications when some experience has been gained. Lower side-slopes can be used at a later stage for cleaning up the final mineral fractions—see below.

Use the mechanical vibrator and a moderate feed rate to process the SPT sink heavy mineral fraction through the Frantz in a number of steps, increasing the current at each stage. The exact number of passes depends upon the nature of the sample and can be varied with experience. After each stage, the least magnetically susceptible sample should be reprocessed. Four passes using current (*A*) settings of 0.4, 0.8, 1.2 A and full-scale (1.6 A) are usually adequate for titanite-bearing samples. Fewer steps can be used if no titanite is present in the 0.4 or 0.8 A fractions. Minerals that typically behave magnetically at various current settings are listed in Fig. 2.1.

Titanite will often separate out in the magnetic fraction at 0.8 and 1.2 A, but may be contaminated with a variety of minerals, e.g. amphibole and pyroxene. In general, playing around with different current settings, slope and tilt, may provide a relatively clean separate. Otherwise handpicking may be used. Another DIM step may also be useful.

Apatite and zircon tend to separate out on the non-magnetic side following the four passes outlined above. To clean up the apatite fraction, reduce the side-slope on the Frantz to +5° and run at full-scale current, then at +2°, but note at slopes less than +2°, some apatites behave magnetically. To clean up zircon, reduce the side-slope on the Frantz to −2° (top towards front) and run at full-scale current. This should be done in gradual steps, i.e. +5° then 0° to −1°, then if still dirty −2°. This procedure can remove sulphides,

aluminous titanites (grothite) and metamict zircons, but is not always successful.

After completing routine separations for apatite and zircon, other minerals can still contaminate these fractions. In the apatite fraction, these include:

(a) Barite—often occurs in cuttings samples from oil wells where barite has been used in the drilling mud. Barite contamination can be avoided if cutting chips are washed and are large enough so that they can be sieved to retain the >500 μm fraction. This fraction is then ground and processed in the usual way.
(b) Fluorite—generally occurs in particular granite provinces, e.g. some S-type granites and tin-granites and in sediments derived from such parent sources. Often such an apatite fraction is unworkable as fluorite has almost identical physical properties to apatite and cannot be separated by any of the usual techniques. However, apatite has very low abundance in such rocks.
(c) Sulphide/quartz composite grains—because of their composite properties these may be very difficult to handle. As the composites tend to be larger than the apatite, such separates can sometimes be cleaned up using a small nylon of 200 or 300 μm sieve size. Otherwise handpicking may be the only way to remove such grains.

In the zircon fraction, the contaminants may include non-magnetic sulphides. If sulphide grains are large, then first sieve in the same way as for apatite (see above). Otherwise dissolve sulphide in aqua regia in a small beaker under a heat lamp. This may need to be done several times to remove all the sulphides. The recovered grains will then need to be subjected to a further heavy liquid separation (e.g. SPT) in order to remove the light minerals liberated from the sulphide composite grains.

DIM is typically used in the last stage of the mineral separation treatment to separate apatite (floats) from zircon and titanite (sink) (see Fig. 2.1j).

Volcanic glass is usually separated using a Frantz® Isodynamic Magnetic Separator. Bubble junction glass shards form the best surfaces for counting fission tracks and are weakly magnetic and separate out between 1.2 and 1.6 A with side-slope between 5° and 10°. Pumiceous glass, which is slightly more magnetic, is often vesicular and does not usually provide an ideal surface for counting fission tracks. Note that volcanic zircons often have glass overgrowths that may cause them to float in heavy liquids. To dissolve the glass so that the zircons sink, as would be expected from their density, the heavy mineral concentrate should be soaked in concentrated HF for 1–3 min (care being taken not to inadvertently dissolve other minerals of possible interest).

2.4.3 Further Possible Final Treatment

The last three steps shown in Fig. 2.1 (steps i–k) can be used selectively coupled with handpicking, especially if only a small amount of heavy and non-magnetic fractions remained after step (h).

Step i involves an additional heavy liquid separation method for further purifying and reducing sample size. This can be achieved by centrifuging a mixture of the non-magnetic mineral fraction, which formed the sink fraction in SPT (at a density of 2.85 g/cm^3), in a further solution of SPT made up to a maximum achievable density of ~3.10 g/cm^3.

A final sieving step k is often useful for FT grain mount preparation by concentrating an optimal grain size. This involves sieving a small volume of grains using either small brass sieves or disposable sieve cloths (e.g. nylon bolting cloth) secured over small plastic cups. The range of grain sizes present in a mineral separate depends on a variety of factors and is highly variable, but typically the most suitable grains for FT analysis will fall in the range of ~80–300 μm. However in any particular separate, the largest grains will generally be the most suitable for providing large clear areas for analysis, so further subdivision into a more restricted size range may be desirable. In addition, the ideal scenario for a grain mount is that all grains are ground and polished to a desired internal surface. Working with mineral separates of similar size allows all grains to attain a common surface/depth during grinding and polishing. However, final sieving should be carried out carefully because for some studies, such as on detrital grains; it may bias the representation of different populations (see Chap. 16, Malusà 2018).

2.5 Sample Mounting and Polishing

Prior to carrying out this step, if (U-Th)/He dating is also planned for the sample, then it is recommended to first handpick the best-quality grains (in terms of size, shape and clarity) from the final mineral concentrate for that purpose, as grain morphology requirements for FT analysis are less stringent.

The aim of the different steps described in this section (see Fig. 2.2) is to establish a flat and well-polished surface, in an appropriate crystallographic orientation, that results from the removal of sufficient external grain material to expose an internal grain surface for analysis (i.e. 4π geometry—see Wagner and van den Haute 1992, and Chap. 1, Hurford 2018).

It is important that care be taken at every stage of sample and mount preparation to produce the best-quality

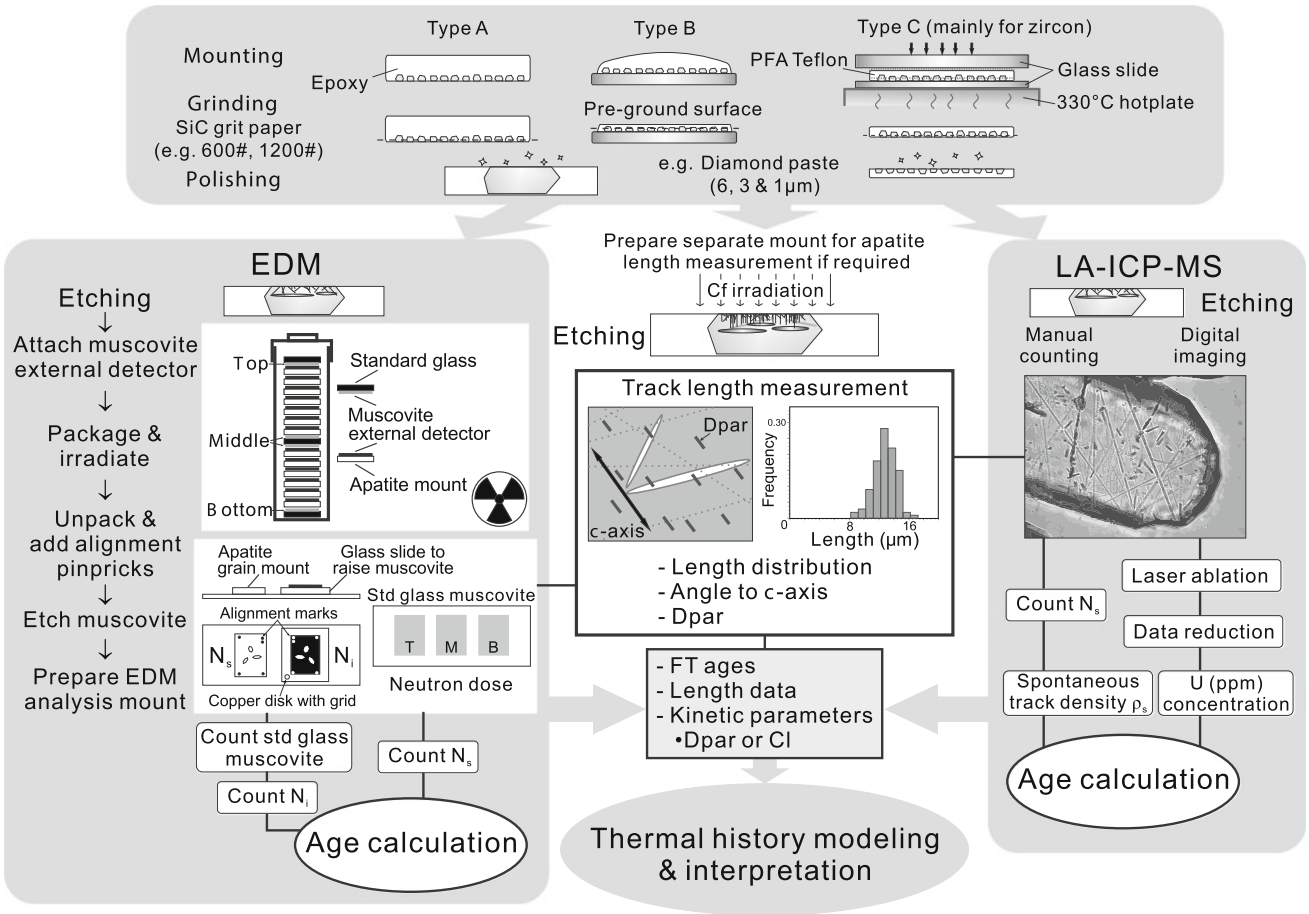

Fig. 2.2 Alternative methods for preparing and collecting data from mineral separates for FT analysis using the External Detector Method (EDM) and LA-ICP-MS protocols, as well as the measurement of track lengths and a kinetic indicator in apatite, either Dpar or Cl. Dpar is measured parallel to the crystallographic *c*-axis. On grain mount N_s = spontaneous fission tracks counted on grain mount and N_i = induced fission tracks counted on mica detector, ρ_s = the spontaneous fission-track density (tracks/cm^{-2}) calculated from N_s. See text for further information

polished surface. Polishing time is variable for individual samples, so it needs to be monitored periodically. Proper washing between each polishing stage is also crucial for preventing cross-contamination between different grades of diamond paste or any other polishing media used, e.g. alumina powder, colloidal silica or other suspensions. Factors contributing to poor polishing outcomes may include cracking of grains induced by rock crushing, inadequately mixed or cured resins and grain shatter during grinding. Over-grinding and polishing (leading to the production of excessive relief) should be avoided. Grinding the grains too thinly or leaving insufficient thickness of mounting media to secure the grains may result in grains falling out during polishing or etching, and lead to contamination or damage of polishing laps.

2.5.1 Apatite

Mounting A wide variety of epoxy resins suitable for making apatite or volcanic glass mounts are available. It is important to follow the manufacturer's instructions exactly with respect to the resin-to-hardener ratio, curing time and temperature. Improperly set epoxy may result in a soft or gluey texture after curing and lead to cracking of grains and contamination of polishing laps, as well as some grain loss.

There are several different mounting media available. Two suitable resins are EpoFix™ (from Struers) for mounting at room temperature and Petropoxy 154™ (with very low volatility and toxicity, available from Burnham

Petrographics) for mounting at elevated temperature (suggested at 135 °C on a hotplate). Using these resins, one can either make an epoxy-only button (type A in Fig. 2.2) or mount the grains directly on glass (type B in Fig. 2.2). Many laboratories prefer the latter and use cut-down mounts on glass, so they can fit into irradiation cans for neutron irradiation for the EDM protocol. For LA-ICP-MS, samples are mounted directly on either an epoxy-only button or glass slide without the need for modification of the slide. Volcanic glass is usually mounted in an epoxy resin (cold setting) button mount and ground and polished in a similar manner to apatite.

Grinding and Polishing Grains in type A mounts are already exposed at or near the surface, whereas grains in type B mounts are fully enclosed within the epoxy. Both types of mount can be further processed by grinding manually with SiC grit paper (e.g. 1200# or 600#) on a glass plate before polishing on a rotating lap with different grades of diamond paste (e.g. 6, 3 and 1 μm). However, an extra time-saving pre-grinding step for type B mounts is to directly expose target grains prior to SiC grinding by using an automatic cut-off machine (e.g. Struers Accutom™), if available.

2.5.2 Zircon and Titanite

The use of FEP Teflon (type C in Fig. 2.2) for mounting zircons for etching was developed by Gleadow et al. (1976). However, during long periods of etching, as required for zircons with low radiation damage, grains often tend to fall out. Following work by Tagami (1987), many laboratories changed over to PFA Teflon. This Teflon has a higher melting temperature and maintains its transparency even after prolonged etching. For mounting with PFA Teflon, it is recommended to use quartz glass or a release agent, as it is often difficult to remove the Teflon sheet from other types of glass slides. One issue with PFA Teflon, however, is that it is often sold in bulk and may be more difficult to access commercially.

Tagami (2005) described the mounting, grinding and polishing of zircon in some detail. Of special note is the following:

- Teflon should not be allowed to overheat and create bubbles, which will ruin the mount.
- As zircons are exposed at the surface of the Teflon, very little grinding is necessary. Start with SiC grit paper (e.g. #600 or #1200) on a glass plate and only sand about 2–3 times over each before using different grades of diamond paste (e.g. 6, 3 and 1 μm) or some other medium on a rotating lap. There is no actual adhesion between the Teflon and the zircons, so over-grinding is a common cause of grains falling out of Teflon mounts during etching as it removes the small Teflon lip, which encloses and holds the grains. Removal of all the original shine from the Teflon surface is an indication that grinding is nearing an end.
- Titanite may also be mounted in Teflon, but is most commonly mounted in an epoxy button mount as described for apatite above.

2.6 Chemical Etching

Spontaneous fission tracks are revealed by chemical etching in a track-recording material because the etchant preferentially attacks the highly disordered material in the core of the track (e.g. Fleischer et al. 1975). The bulk-etching rate in minerals is not uniform and varies in different crystallographic directions, so that the tracks take on different shapes and sizes, depending on which crystal surface they are etched (e.g. Wagner and van den Haute, 1992). Common etching recipes for different minerals are outlined in Table 2.2.

Apatite and zircon grains are often prismatic and during mounting often tend to align on prismatic faces, which are approximately parallel to the *c*-axis. This is the orientation sought for optimal track revelation for FT dating (e.g. Wagner and van den Haute 1992; Gleadow et al. 2002; Donelick et al. 2005; Tagami 2005). In apatite, zircon and titanite etching is anisotropic (i.e. tracks are revealed preferentially parallel to the crystallographic *c*-axis but also need to be fully revealed perpendicular to that axis for etching to be judged as being optimal), and this is particularly evident in low-radiation damaged grains (e.g. Gleadow 1981). In glass, fission tracks have a circular or elliptical cross-section, even after prolonged etching, because the host material etches isotropically (e.g. Dumitru 2000, see also Chap. 1, Hurford 2018).

Over or under etching may jeopardise the quality of data obtained. The correct etching time in minerals, such as zircon and titanite, is highly variable and will depend on a variety of factors, especially the general radiation damage level, which is reflected in the track density. The particular choice of etchant used is also important in many cases. The anisotropic etching characteristics of both zircon and titanite are significantly greater when using acid etchants shown in Table 2.2 or listed in references cited therein, than for the hydroxide etchants. This can be seen in Fig. 2.3, which shows the same zircon etched in a hydroxide and an acid etchant for comparison. Except where the radiation damage levels are fairly high, therefore, the hydroxide etchants are to be preferred and give better results for both these minerals. It

Table 2.2 Commonly used etching recipes and notes for different minerals and glass

Mineral	Etchant	Conditions	Comments
Apatite	5 N HNO_3 (Gleadow and Lovering 1978)	20 ± 1 °C 20 s	Different HNO_3 strengths have also been reported, e.g. HNO_3 conc for etching time of 10–30 s (Fleischer and Price 1964) and 1.6 M (7 vol.%) at 25 °C (or at room temperature) for 20–40 s (Naeser 1976), but those listed to left are the most commonly used (see also Seward et al. 2000 and Sobel and Seward 2010) Following etching, wash thoroughly under tap, dry with clean paper tissue and leave in air for a few hours to ensure all etchant has dried out from within mount before inspecting under a microscope. If a longer etch is required, wet mount briefly before re-etching. This aids the entry of etchant into partially etched tracks, as normally any extra etching will only be for a matter of seconds
	5.5 N HNO_3 (Carlson et al. 1999, see also Donelick et al. 2005)	21 ± 1 °C 20 ± 0.5 s	
Zircon	Binary eutectic mixture of KOH:NaOH (in proportions by weight: 8.0 g KOH and 11.2 g NaOH—Gleadow et al. 1976) A variant of the eutectic is NaOH:KOH:LiOH (6:14:1), which is reported to increase etching efficiency at lower etching temperatures for comparable etching times (Zaun and Wagner 1985)	225–230 °C 4–120 h (or more)	Vessel: (ceramic, platinum or Teflon)—place on hotplate (monitor temperature with a thermometer) and cover with inverted beaker to prevent crust from forming around top. Check temperature of etchant solution with thermocouple Place zircon mounts face down in etchant (they will float), leave initially for 4 h and then check etching progress. Note—grain surfaces with highest etching efficiency are those showing the presence of sharp polishing scratches Following etching place the mount in 48% HF in a Teflon dish for 15–30 min in order to clean up grains. This will not affect the quality of the etched grains After etching, mounts will almost always deform slightly. In order to flatten the mount so that a muscovite detector with a good contact can be later applied, more heating should be carried out, but not enough to melt the Teflon or push grains further into the mount *Note* Generally the time required for proper fission track revelation in zircon is inversely proportional to the accumulated radiation damage, which is related to uranium concentration and age of the grain. Hence, etching duration varies over a broad range
	For other possibilities, see also Garver (2003) and Tagami (2005)		
Titanite	37% HCl (Naeser and Dodge 1969)	90 °C 15–60 min	Vessel: Stainless steel, Teflon or alkali-resistant ceramic beaker Preparing the acid etchant produces an exothermic reaction, so leave to cool down over night Etching times typically vary between 10 and 60 min, depending on the level of radiation damage (see Fig. 2.4). Check track etching rate and characteristics after 10 min. Before viewing under microscope wash mount thoroughly. Return to etchant to complete etching—repeat as often as necessary with varying times *Note* The anisotropic etching characteristics of titanite are significantly greater when using the acid etchant (especially for low radiation damage grains)—so the NaOH etchant is preferred for such grains. This etch is also suitable for track revelation in garnets and epidote (Naeser and Dodge 1969), but etching time required may be >1 h. A 75 M NaOH etch may be required for etching in some garnet compositions (Haack and Gramse 1972). Over long etching times the NaOH solution may dehydrate and become less efficient, so a condenser may be useful when using this etchant
	1HF:2HCl:3HNO_3:6H_2O (Naeser and McKee 1970)	20 ± 1 °C 10–60 min	
	50 M NaOH solution (40 g NaOH: 20 g H_2O) (Calk and Naeser 1973)	130 °C 10–60 min	
Muscovite	HF (Fleischer and Price 1964); strengths of both 48 and 40% have been reported	20 ± 1 °C Reported: 5–45 min Commonly used: 20–25 min	Vessel: Teflon dish After etching, wash muscovite thoroughly in warm running water. Then place the muscovite on a glass slide on a hot plate at ~100 °C to drive off any HF absorbed between the cleavage planes, this will prevent any later inadvertent etching of the microscope objective
Glass	HF (Fleischer and Price 1964), different strengths ranging from 48 to 12% have been reported	23 °C 5–90 s depending in part on acid strength	Vessel: Teflon dish After etching, neutralise HF and wash mount thoroughly in warm running water *Note* obsidian usually takes longer to etch than glass shards

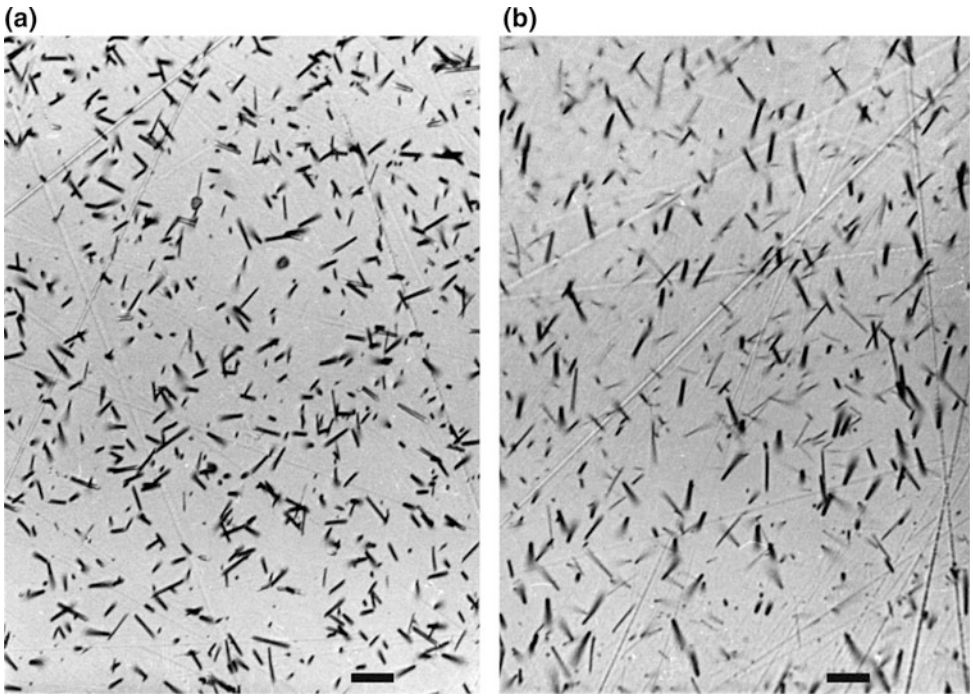

Fig. 2.3 Spontaneous fission tracks in zircon from the Mud Tank Carbonatite in Central Australia etched in **(a)** the KOH:NaOH eutectic etchant of Gleadow et al. (1976) and **(b)** in the equivolume HF:H_2SO_4 etchant of Krishnaswami et al. (1974). The eutectic etch has revealed the tracks more isotropically than the acid etchant and is the preferred etchant for zircon. The polished surface is parallel to the (010) cleavage, and the extended faint lines running across each frame are polishing scratches. The scale bar on each frame is approximately 10 μm

is extremely important in these minerals that the degree of etching be judged from the appearance of the tracks and not from the application of some standard etching time (Fig. 2.4). Increased radiation damage results in markedly shorter etching times required to fully reveal tracks for microscope observation (Fig. 2.5). Hence, it is common practice, especially when working with sediments, to prepare more than one mount of a zircon and titanite grain population and etch for different times in order to enable FT analysis to be performed on the entire population (Naeser et al. 1987). For strategies on handling zircons with very-low or very-high fission-track densities, see Appendix in Naeser et al. (2016).

Because radiation damage does not accumulate to any degree in apatite, it is more consistent in its etching behaviour and a standard etching time is commonly used, although exceptions will be found from time to time. However, for most apatites, it is important to adhere to a strict etching protocol, so that key parameters such as track lengths and Dpars (see Sects. 2.11.5 and 2.11.7) can be measured in a consistent fashion and reproduced in other laboratories.

2.7 The External Detector Method (EDM)

The most common protocol for studying minerals with heterogeneous uranium content between different grains is the External Detector Method (EDM). In order to determine their ^{238}U content, the EDM requires that etched grains be sent to a nuclear reactor for thermal neutron irradiation. The sequence of steps involved in preparing samples for irradiation for a number of minerals has been described in some detail in a number of works cited in Sect. 2.2 (see also figures in Gleadow et al. 2002 and Tagami and O'Sullivan 2005) and is shown in Fig. 2.2.

Briefly, the spontaneous fission tracks are etched on an exposed internal polished surface on the grains and the induced tracks on a muscovite external detector attached to the grain surface during neutron irradiation. After irradiation, the external detector is etched to reveal an induced fission-track mirror image corresponding to grains in the mount (Chap. 1, Hurford 2018).

Even though this results in a second set of tracks being produced within the grains themselves, these tracks will not be detected because they are not etched after the irradiation. Also, because ages can be measured on individual grains, a careful selection of grains can be made to avoid those which may be badly etched or contain dislocations. The external detector is usually a sheet of low-uranium muscovite (commonly Brazil Ruby—with ASTM Visual Quality of V-1, which is designated as clear and free of stains and inclusions, cracks, waves and other defects, with about 5 ppb uranium). Suitable high-quality muscovite external detectors can be bought commercially already cleaved to ~45–55 μm thickness and pre-cut to a suitable size (typically ~12 × 12 mm). Muscovite is more suitable as a detector in dating applications than plastics, such as Lexan, because its track registration and etching properties are much more like those of the minerals with which it is being compared.

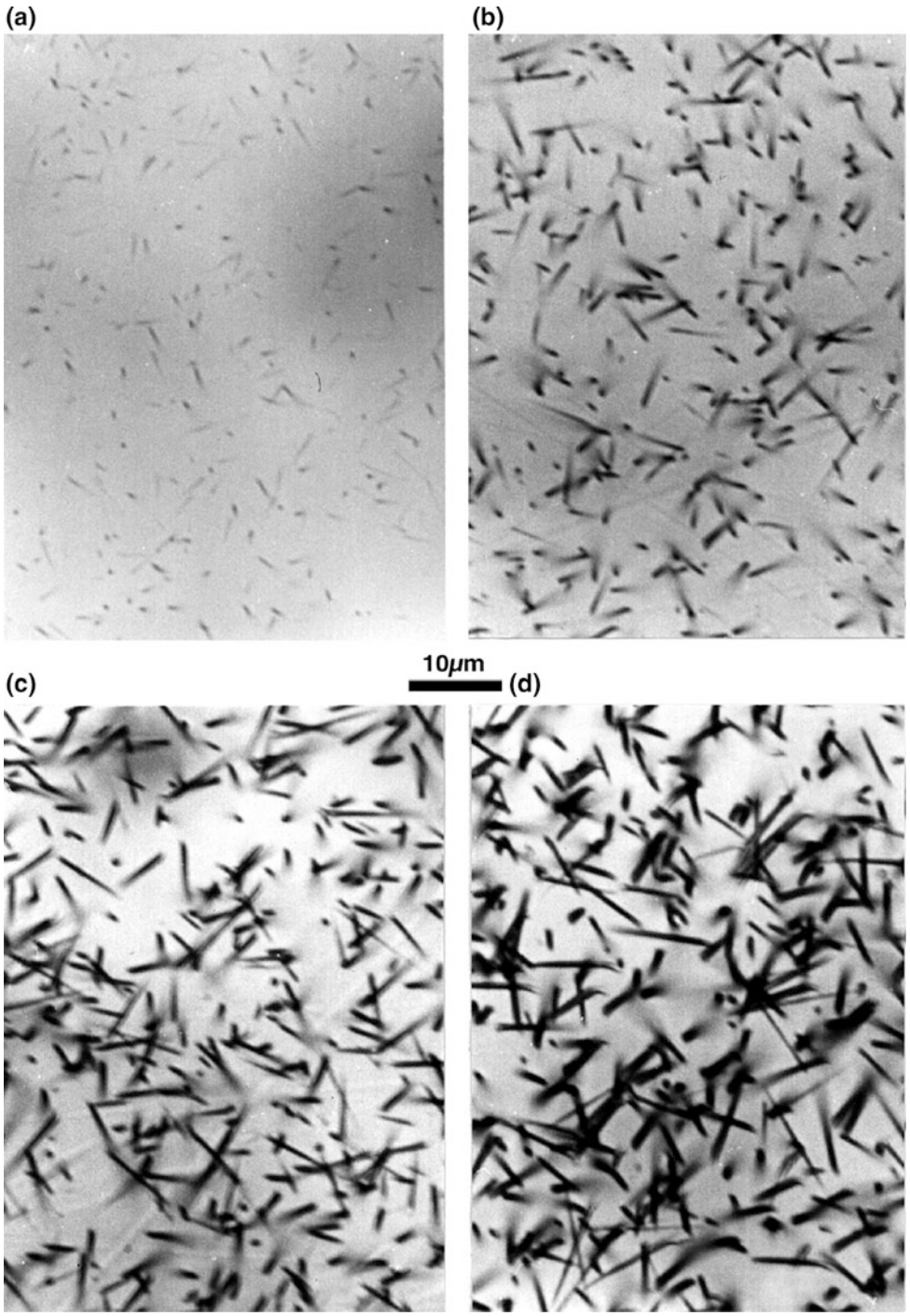

Fig. 2.4 Spontaneous tracks in titanite following various etching times; **(a)–(d)** show tracks etched for 5, 10, 15 and 20 min, respectively, in the mixed acid etchant ($1HF:2HCl:3HNO_3:6H_2O$). The tracks in **(b)** represent the minimum degree of etching for which a reliable track density can be obtained

To measure the FT age by the EDM involves determining the spontaneous track density in a selected grain and finding the mirror image area on the muscovite external detector where the induced track density is counted over exactly the same area. Because the geometry of track registration is not the same for the internal surface (4π) on which the spontaneous tracks are measured and the external detector surface (2π) used for induced tracks, a geometry factor must be introduced to correct for this difference (e.g. Wagner and van den Haute 1992). The geometry factor is ~ 0.5, but this is not exact because of small differences in detection efficiency of the two surfaces and differences in the range of fission tracks in the two different materials (e.g. Iwano and Danhara 1998; Gleadow et al. 2002). A consequence of anisotropic etching rates in minerals such as zircon or titanite is that some grain surfaces in a mount may have a low etching efficiency (e.g. Fig. 2.4). Comparison of spontaneous tracks on such surfaces with induced tracks in an

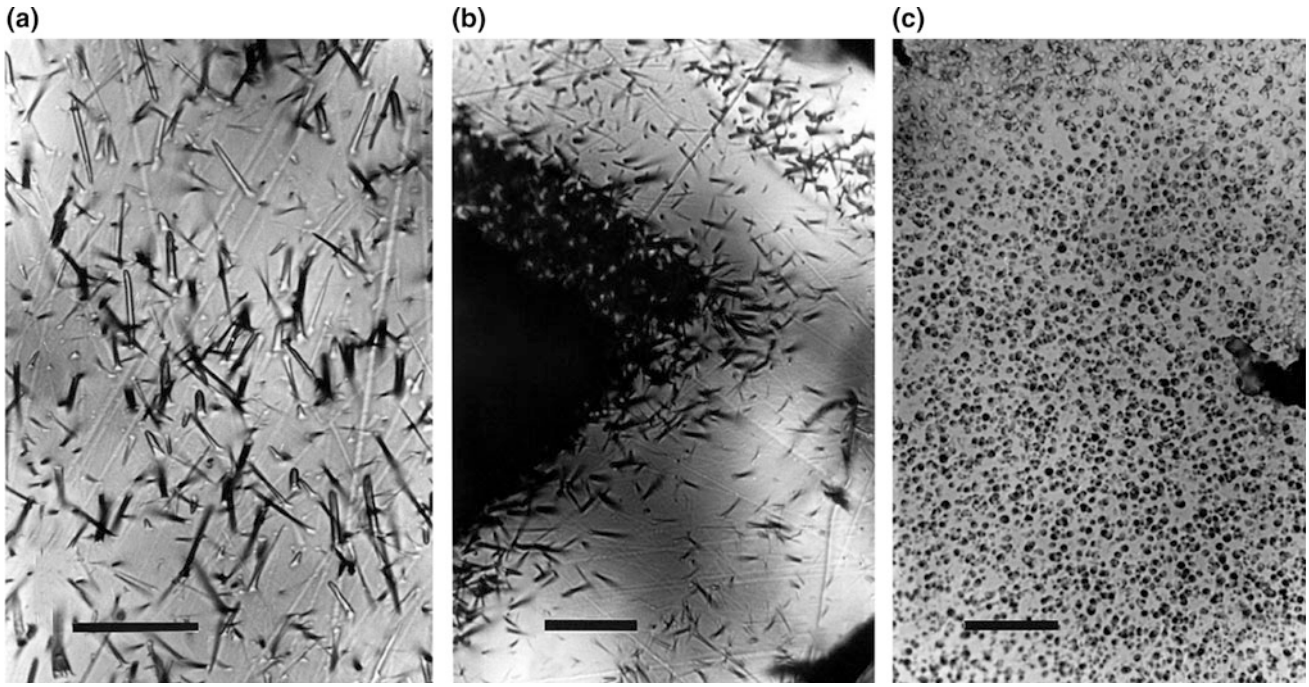

Fig. 2.5 Etching of titanites at different stages. **a** Shows the highly anisotropic etching of induced tracks in annealed titanite, etched 25 min in the 1HF:2HCl:3HNO_3:6H_2O etch at 20 °C (see Sect. 2.6). **b** Shows the less anisotropic but very variable etching at intermediate radiation damage levels in a zoned titanite, ranging from under etched in low U zones, to strongly over etched and unresolvable in the highest-uranium core zone (etched 12 min). **c** Shows the small rounded, conical etch pits, which resemble tracks in glass, found in titanite with an extreme track density of $\sim 8 \times 10^7$ cm^{-2} and etched for 1 min. The scale bar is 20 μm in each case

adjacent muscovite detector, where the etching efficiency approaches 100%, will clearly give erroneous results. A very careful selection of only the highest etching efficiency surfaces, as identified by sharp polishing scratches (Figs. 2.3, 2.5a) (e.g. Gleadow 1978), is therefore essential for the EDM. Care is also necessary when dealing with low track densities in minerals that etch anisotropically to ensure that etching has been sufficient for even the most weakly etched tracks to be revealed (see Fig. 2.3). In some samples, such as young zircons or titanites, it is extremely difficult to reveal tracks in certain orientations. This effect is moderated by accumulated radiation damage so that most zircons and titanites with track densities between $\sim 10^5$ and 10^7 cm^{-2} can be readily analysed by the EDM (Gleadow 1981, see also Naeser et al. 2016—Appendix 1). Montario and Garver (2009) developed a scanning electron microscope technique, which permits counting of track densities to as high as 2 $x10^8$ cm^{-2} allowing for a greater range of high track density zircons to be counted, particularly in populations containing very old (Precambrian) grains, which had previously been considered uncountable.

Also noteworthy is a further method complementary to the EDM for FT dating of moderate-to-high uranium zircons carried out by electron probe microanalysis (EMPA). This method involves determining uranium concentration and imaging of the number of spontaneous fission tracks intersecting the surface, using an electron backscatter detector (Gombosi et al. 2014). Dias et al. (2017) reported an alternative approach to FT dating of zircons, but also using EMPA to measure uranium concentration.

Because of its relative ease of handling, amenability to automation (see Sects. 2.11.4 and 2.12) and its provision for single-grain age information, the EDM is currently the preferred dating method for apatite, zircon and titanite in most FT laboratories.

2.7.1 Preparing Mounts for EDM Age Dating and Neutron Irradiation

2.7.1.1 Wrapping and Packing for Irradiation

- Cut down etched apatite mount size to fit into the irradiation can (e.g. 1 × 1.5 cm) and thoroughly clean with soapy lukewarm water and dry in alcohol.
- Overlay mounts with dust-free pre-cut (if possible) low-uranium muscovite—always handle with tweezers. A clean muscovite surface may be formed by placing it on a piece of sticky tape and lifting off a thin flake of muscovite. To ensure a good contact with grains during irradiation make sure that the muscovite does not extend beyond edges of the mount.

- Prepare heat shrink plastic bags with an opening sufficient to slide the muscovite and grain mount pair in easily.
- Place muscovite–mount pair inside the bag and holding contents firmly with tweezers. Use a kitchen-type bag sealer, to close the opening as close as possible to the muscovite–mount. Trim the edges of the bag to provide passage for escaping air. Heat two clean glass microscope slides on a hotplate at 100 °C. Place bag and its contents on one slide keeping the muscovite face up and cover immediately with the other slide. Press firmly with tweezers to achieve good contact. Some laboratories use low chlorine-content reactor-friendly Scotch 3M® magic tape or Parafilm M to affix the muscovite to the mount.
- Wrap the standard glass–muscovite pair in the same way as described above.
- Place mounts in an irradiation can and record order of samples in the stack. The number of samples that can be fitted into an irradiation stack will depend on local reactor protocols. Use two standard glasses in each irradiation package one at top and bottom of the stack, to monitor any spatial neutron flux gradients. A further glass standard may also be inserted in the middle of the package (Fig. 2.2). If possible, it is also recommended to include an appropriate mineral age standard (e.g. Durango apatite or Fish Canyon Tuff zircon) within the irradiation package (see Chap. 1, Hurford 2018).
- If the irradiation can is sucked pneumatically into the reactor to the irradiation position, it may be necessary to allow for the addition of packing material at each end of the can (e.g. Al foil padding), which acts as a shock absorber preventing glass breakage on impact.
- *Note*: Irradiation results in significant levels of radioactivity due to short-lived isotopes, mainly related to Na content present in conventional soda lime petrographic glass slides, but also from sweat in fingerprints (*so gloves should always be worn when preparing material for irradiation*). In this respect, silica glass slides are less problematic.

2.7.1.2 Standard Glasses

Hurford and Green (1983), Wagner and van den Haute (1992) and Bellemans et al. (1995) provided information on different glass standards and evaluations of their suitability for monitoring neutron fluence and determining ^{238}U content of individual grains. In the early years of FT dating, glasses produced by the National Institute of Standards and Technology (NIST) (Carpenter and Reimer 1974) the SRM-series were commonly used for monitoring. However, these are depleted in ^{235}U and contain a variety of trace elements, and have gradually been replaced by the Corning CN1–CN6 series with a natural ^{235}U/^{238}U ratio and fewer trace elements (see Bellemans et al. 1995). CN1 and CN2 are generally suitable for zircon and titanite and CN5 for apatite. However, worldwide stocks of CN5 have now been exhausted, but uranium-doped oxide glass IRMM-540R (15 ppm uranium) produced by the European Commission's Institute for Reference Materials and Measurements (IRRM) has proven to be an effective substitute (De Corte et al. 1998). Further, uranium oxide-doped glass IRMM-541 (50 ppm uranium) is suitable as an alternative standard, e.g. for zircon and titanite, which require shorter irradiation times due to their generally higher uranium content.

The use of induced tracks in muscovites over standard glasses has been instrumental in acquiring zeta (ζ) calibrations based on the analysis of geological age standards analysed by other geochronological techniques (Hurford and Green 1983; Chap. 1, Hurford 2018). This procedure settled earlier disagreements about the ^{238}U spontaneous fission decay-constant, neutron dosimetry calibrations and ambiguities in corrections for measuring spontaneous and induced fission tracks on different surfaces and in different materials, and was deemed to be a workable solution to some long-standing problems (Hurford 1990). The ζ-method calibration is the most widely used for age determinations in FT laboratories today. But this method also has some drawbacks because it yields calibration factors that are to some extent personal, vary for different mineral species and combine known and unknown factors (e.g. Wagner and van den Haute 1992; Hurford 1998). An alternative procedure to using standard glasses, but not that widely used, is the ϕ-method. This involves an absolute determination of the thermal neutron fluence by measurement of neutron-induced gamma activity in Au and Co metal activation monitors included in irradiation cans together with samples (e.g. van den Haute et al. 1998; Enkelmann et al. 2005).

2.7.1.3 Neutron Irradiation

In a nuclear reactor, the total neutron flux may comprise three neutron components of different energy ranges; fast, epithermal and thermal. When choosing a reactor for sample irradiation, it is crucial that only a well-thermalised neutron facility is used (e.g. Wagner and van den Haute 1992). This is required in order to avoid track production by epithermal neutrons from ^{235}U fission or by fast neutrons from ^{238}U and ^{232}Th fission. Such tracks would be indistinguishable from the thermal neutron-induced ^{235}U fission tracks required. Since the Th/U ratio of material used for FT analysis is highly variable, it is important that the nature of the neutron flux in the irradiation position used is well known. Ratios of thermal/epithermal and thermal/fast neutrons of >100 and >80, respectively, provide some certainty that practically all induced tracks measured in muscovite external detectors originate from ^{235}U fission (see Green and Hurford 1984 and Wagner and van den Haute 1992 for further details).

The integrated neutron dose requirement for different minerals varies and is dictated by the expected uranium content of a particular mineral. Typical nominal doses requested for the most common minerals used for FT studies at the University of Melbourne in past years have been apatite $\sim 1 \times 10^{16}$ n cm^{-2}, zircon $\sim 1 \times 10^{15}$ n cm^{-2}, titanite $\sim 4–5 \times 10^{15}$ n cm^{-2}. These values are not absolute, however, as the fluence requested in relation to that actually received and monitored within the irradiation package may vary from reactor to reactor.

2.7.1.4 Post-irradiation Sample Handling and Slide Preparation

- After the irradiated package is received, place it in properly lead-shielded storage until radiation levels, which should be monitored periodically, are safe and samples can be unpacked.
- Prior to unwrapping samples, use a sharp pin to make holes in each corner of the glass–muscovite pair making sure that one corner has two holes.
- If tape is used to secure muscovite to glass mounts, remove very gently so as not to lift off large amounts of muscovite flakes or alternatively cut around the detector with a scalpel and place in etchant and any remaining tape will fall off.
- Etch muscovites in HF as listed in Table 2.2.

Each apatite, zircon and titanite grain mount and muscovite can be mounted together on a standard petrographic glass slide (typically 26 × 76 × 1.5 mm) so that one is the mirror image of other. These can be mounted using a small amount of Petropoxy® 154, but note that in cases where grains are embedded in Teflon, then these may be mounted using double-sided sticky tape. To minimise focussing requirements during track counting the mica should be glued on a thin glass slide to bring it to the same level as the grain mount. Ensure that the sample number is labelled on the back of the slide. A reference point should be placed in the centre of the mount, between the grain mount and muscovite. The most convenient is a metal (copper) disc with grid (used for locating and referencing specific areas in Transmission and Scanning Electron Microscopy), which is used as a central coordination point for commencing the later alignment procedure keyed to the pin-pricks between specific grains and their mirror image on the muscovite (see Fig. 2.2 in Sect. 2.11.4). Such coordination points can also be used later for locating the exact grains on which track measurements have been carried out for electron microprobe analyses if required (see Sect. 2.11.7).

2.8 The LA-ICP-MS Method

LA-ICP-MS is the first technique that has been able to compete with the traditional neutron irradiation method for determination of ^{238}U content in terms of high spatial resolution and ppm sensitivity. This analytical development has added a new approach for FT analysis, whereby ^{238}U can be determined directly in mineral grains, rather than by using ^{235}U-induced fission tracks as a proxy, as required by the EDM. LA-ICP-MS facilities are now becoming widely available, and this mode of analysis has considerable advantages over the conventional EDM, as it no longer requires neutron irradiations and the long delays in sample processing (typically many weeks) that they require. Other advantages of this approach are that it eliminates the need for handling radioactive materials and as only one track density measurement (the spontaneous FT density) is required, it reduces the overall requirement for FT counting (e.g. Hasebe et al. 2004; Donelick et al. 2005; Vermeesch 2017, and Chap. 4, Gleadow et al. 2018).

Hasebe et al. (2004) carried out the first systematic study using LA-ICP-MS for FT analysis, an approach foreshadowed by Cox et al. (2000) and Košler and Svojtka (2003). More recent studies by Donelick et al. (2005), Hasebe et al. (2009, 2013) and Chew and Donelick (2012) have provided additional experimental details and demonstrated the effectiveness of this approach.

The sequence of steps using LA-ICP-MS is illustrated in Fig. 2.2. The first three steps are the same as for the EDM, in that a grain mount is prepared, polished and then etched to reveal the spontaneous fission tracks. However, prior to mount preparation, it is important to confirm that the mount size can be accommodated by both the microscope stage and laser cell, as each laser cell may have specific sample dimension requirements. The spontaneous tracks are then counted manually or on sets of digital images that are acquired using an automated image capture system referenced to a coordinate system best defined by three metal discs with grids placed around the grain mount (see Sect. 2.12 and Chap. 4, Gleadow et al. 2018). The grain coordinates and the slide are then transferred to the laser ablation cell and analysed by LA-ICP-MS. Most studies conducted have used a single ablation spot of $\sim$20–30 μm diameter or a rastered scan centred around the area where the tracks were counted. As all of the tracks, which are etched on a surface in zircon and apatite, originate within $\sim$5.5–8.5 μm of the surface, respectively (e.g. Hasebe et al. 2009), it is important to ablate the surface only to about that depth, in case there is zoning of uranium in the vertical dimension.

The ^{238}U concentration is determined relative to suitable external standards of accurately known and uniform uranium abundance (e.g. NIST610 and 612 glasses) and measurement of an appropriate internal standard, e.g. ^{43}Ca (apatite), ^{29}Si (zircon), to correct for variations in ablation volume (e.g. Hasebe et al. 2004, 2009, 2013; Chew and Donelick 2012). These works also list operating conditions, but these are by no means universal and may vary with specific instrumentation used.

LA-ICP-MS for direct determination of ^{238}U is a relatively new approach to FT analysis. It is usually calibrated using a variant of the zeta calibration approach (Hurford and Green 1983; Donelick et al. 2005) or can be calculated as an absolute age using explicit values for all the constants in the age equation (e.g. Hasebe et al. 2004; Gleadow et al. 2018). Efforts are also underway to identify some well-characterised and matrix-matched minerals with relatively homogeneous uranium content to correct for elemental fractionation during laser ablation (e.g. Soares et al. 2014; Chew et al. 2016). Vermeesch (2017) has outlined the statistical treatment of analytical uncertainties arising from different approaches to LA-ICP-MS-derived FT age dating (see also Chap. 6, Vermeesch 2018).

As outlined earlier, the measurement of ^{238}U by LA-ICP-MS is a relatively new approach to FT dating. To date, mainly LA-ICP-MS data on apatite, zircon and volcanic glass have been reported and sample preparation is similar to that described previously for these minerals.

2.9 Double–Triple-Dating

With technological advances in instrumentation and an improved understanding of the behaviour of different geo-thermochronological systems, it has become possible to carry out dating of individual grains from an aliquot using independent isotopic systems, i.e. combinations of FT, U/Pb and (U-Th)/He analyses on either apatite or zircon. This so-called double- or triple-dating approach is a powerful new development in the geo-thermochronology toolbox because the radioactive decay schemes for these systems have different temperature sensitive ranges and can provide more robust constraints for computing time–temperature histories (Chap. 5, Danišík 2018).

Earlier approaches using different combinations of methods on subsets of particular sample aliquots were prepared for analysis using standard procedures (e.g. Carter and Moss 1999; Carrapa et al. 2009). When using FT dating in combination with other techniques on single grains, principally by use of LA-ICP-MS, some modification of practical steps may be required in sample preparation. Chew and Donelick (2012) described the double-dating of apatite using the FT and U-Pb methods on single grains, while Hasebe et al. (2013) also outlined a similar approach for dating both apatite and zircon. As all the data (apart from the counting of spontaneous fission tracks) in both studies were acquired using LA-ICP-MS, the preparation of mounts was essentially similar to that described in Sects. 2.5 and 2.6 above. For triple-dating (U/Pb, FT and U-Th/He) of apatite (Danišík et al. 2010), analyses were carried out on subsets of an exceptionally large apatite aggregate precipitated in cavities and veins in a late Palaeozoic rhyolite; therefore, the standard method was used for the preparation of samples for each dating method. Reiners et al. (2007) reported a combined apatite FT and (U-Th)/He double-dating study. In this case, the apatite FT age was determined by conventional mounting in epoxy and counting of spontaneous FT density (ρ_s) and uranium content determined by LA-ICP-MS on the same grains, following which grains were plucked from the mount and dated by standard (U-Th)/He procedures.

Note: With ongoing technical developments, apatite FT dating might in the future be combined with in situ (U-Th)/He dating, in which case samples will need to be embedded in Teflon, due to the excessive degassing of epoxy mounts preventing the attainment of the ultra-high vacuum required (e.g. Evans et al. 2015). A similar mounting procedure would also be applicable to double- or triple-dating of zircon grains in such an in situ (U-Th)/He dating approach.

2.10 Microscope Requirements

The microscope is the single most important component in a FT dating laboratory, but the choice of equipment is frequently not given the scrutiny it deserves. Any old microscope will not do. What is required is a research-grade microscope of the highest quality fitted with objectives, condenser and illumination to give optimum performance at the highest magnifications (at least 1000×). Polarising equipment and a rotating stage are not necessary for track counting and place significant restrictions on the other equipment that can be used on a microscope. Also, most other microscope stages are more robust and have superior mechanical slide movements than do rotating stages.

For work at high magnification, it is important to have high intensity illumination available and preferably a light source of 50 W or more. In recent years however, illumination for optical microscopy using light-emitting diodes (LEDs) has shown considerable promise as a spatially and temporally stable and cost-effective technology compared to traditional arc lamp illumination sources. It is essential to have both reflected and transmitted light illumination available on the microscope, arranged so that the user can readily switch back and forth between the two. Tracks are usually counted in transmitted light, but reflected light can be useful for resolving complex track overlaps, locating the end of

tracks which intersect the surface, and for counting very-high track densities. Reflected light can also be very useful for locating horizontal confined tracks used in length measurement (see Sect. 2.11.5).

In general, it is more important to have flat-field objectives, such as planachromats, than those that have a very high degree of colour correction. However, some lenses rate highly in both characteristics. Objectives should be parfocal with each other, and it is more convenient if they are mounted in a multiple revolving nosepiece rather than on an individual bayonet-type objective carrier.

An important question is whether to use dry or oil-immersion objectives for the highest magnifications. This is partly a matter of personal choice and both systems are in routine use in FT laboratories. Technically, oil-immersion objectives have superior resolution but other effects often outweigh this advantage. Very fine images are obtained under oil immersion in zircon and titanite, which both have high refractive indices. However, in some other minerals, oil has distinct disadvantages because the refractive index of the usual immersion oil, 1.515, is almost the same as that of the mineral. In apatite and muscovite, this results in tracks losing contrast with the surrounding mineral and becoming more difficult to observe. This problem cannot be avoided by using a different immersion medium because the objectives can only be used with an oil of the refractive index for which they were designed. For this reason, it is often preferable to use dry objectives, which must also be corrected for no cover glasses.

A binocular eyepiece tube is regarded as an essential component of any microscope used for observing and counting fission tracks. The most commonly available eyepieces have magnifications of 10× , although higher magnifications, e.g. 12.5× or 15× are often preferable for FT analysis.

For counting fission tracks, one of the eyepieces should be a focusing type fitted with a graticule, usually in the form of a 10 × 10 grid. In the most commonly used graticules, each grid square is 1 mm across on the carrier disc. For track length measurements, it is essential to have an eyepiece fitted with a scale bar or eyepiece micrometre. Calibration of the scale bar and the area of the graticule are carried out by measuring their dimensions against a stage micrometre, which can be obtained with divisions down to 2 μm. If such a calibration slide is not available, then a satisfactory alternative is to use a piece of optical diffraction grating, although this requires observation under incident light illumination, as the metallic coating of the grating is opaque. Diffraction gratings are accurately ruled with very fine lines, at a known spacing of the order of 1 μm.

Modern research microscopes are all equipped with a sub-stage condenser and field and aperture diaphragms required to produce Köhler illumination (see: http://zeiss-campus.magnet.fsu.edu/articles/basics/kohler.html) for providing the most uniform and optimal specimen illumination across the field of view and the maximum optical resolution for a particular objective lens. It is particularly important to set up the optimum illumination conditions for the particular objective to be used, especially for image capture for automation (see Sect. 2.12). This will almost always be with the 100× lens, the highest lens available.

2.11 Data Collection

2.11.1 Identification of Fission Tracks

In order to count fission tracks, they need to be reliably identified and distinguished from etch pits or features of other origins, such as dislocations or inclusions. Etched fission tracks have certain properties (Fleischer and Price 1964), which enable their discrimination from spurious dislocation etch pits (Table 2.3).

Dislocations are most commonly encountered in large numbers in relatively young volcanic apatites, although they are seldom found in all grains mounted from a single sample. Apatites from slowly cooled plutonic rocks usually show few, if any, dislocations and discrimination is fairly

Table 2.3 Properties that distinguish etched fission tracks from dislocations

Fission tracks
Etched fission tracks: • Straight features, as fission-fragments travel essentially in straight lines • Have a limited length, as fission fragments have a limited range of about 5–10 μm (depending on the host material) and the maximum track length is up to the maximum etched range of both fission fragments and varies from ~10–20 μm in different minerals • Randomly oriented, although highly annealed tracks are preferentially aligned parallel to the *c*-axis in apatite • The distribution of spontaneous tracks must be statistically the same as that of uranium, and hence of induced tracks in a particular material Unetched fission tracks have a limited thermal stability that is characteristic of the registering material and is usually different from that of dislocations or micro-inclusions
Dislocations
• Often bent, branching, curved or wavy • Often occur in swarms, the distribution of which is unrelated to that of uranium (see Gleadow et al. 2002) • Lengths frequently similar to each other and often much greater than those of fission tracks • Often occur with a strongly preferred orientation, either as sub-parallel swarms, or as lines of parallel etch channels • May act as nucleation sites for the precipitation of impurities from the host material, in which case they are readily identified

straightforward. Zircons and titanites tend to have relatively few dislocation etch pits and discrimination is not usually a problem. Zircons may contain minute crystalline inclusions, however that can sometimes be mistaken for tracks, especially where the fossil track density is very low. Often such crystallites show a regular orientation in relation to some crystallographic direction and a range of sizes that can aid in their discrimination.

In general, the problem of discriminating fission tracks from other etch features is not severe, but can become significant when dating grains with very low track densities. It is always an advantage when there are sufficient tracks present so that they can be compared with each other. Experience and an appropriate selection of dating technique are important in handling difficult cases, but it may be wiser to simply go on to another sample.

2.11.2 Counting Techniques

Microscope work for an EDM FT age determination, using the ζ-calibration approach, involves the counting of three track densities: spontaneous (ρ_s), induced (ρ_i) and standard glass (ρ_d). For each of these, the tracks are normally counted at magnifications of 1000× or more, and usually in transmitted light. The depth of focus under these conditions is very limited so that the fine focus of the microscope needs to be moved up and down frequently during counting to follow the three-dimensional nature of each track.

The position of a track in relation to the counting graticule is defined by the intersection of the track with the surface. With experience, this surface-end of the track can be recognised at a glance but at first should be judged from the following characteristics. All the tracks (long and short) will only be in focus together at the surface, so that progressively fewer tracks will be seen as the focus is moved down into the grain. Moving the fine focus up and down can therefore be used to identify the surface-end of the tracks. Also, the intersection of each track with the surface is clearly visible as a dark hole (etch pit) in reflected light (if available). Even in transmitted light, the two ends of a track do not look the same, but can still be identified.

On both the exposed internal grains surfaces and the external detector surfaces, the tracks vary in length from essentially zero up to the maximum for the particular mineral. It is important not to overlook the smallest tracks, or at least to use some consistent criterion as to which of the short tracks will be included in the final track density. Counting the tracks then involves systematically scanning across an appropriate number of eyepiece grid squares, so that each track is included once only. Where the surface intersection of the track lies exactly on a grid line, some consistent convention must be used to assign the track to a particular grid square. For example, a track might be included in a square if it lies along the top or right-hand edge, but not if it is on the bottom or left-hand edge. Further, if no tracks are observed in the grid, then that zero *must* be recorded accordingly and included in the final tally of counted tracks per total surface area analysed. A repositioning technique for achieving more accurate counts of induced tracks in muscovite external detectors in grains with low and/or inhomogeneous uranium concentrations has been described by Jonckheere et al. (2003).

Typically, more than 20 grains should be counted if possible, and the results combined to give an age for the sample. In crystalline samples with complex age spectra or detrital samples, a greater number of grains should be targeted, aiming for about 50–100 grains or even more, as a higher number is especially important for the discrimination of different age populations if present (e.g. Garver et al. 1999; Bernet and Garver 2005; Coutand et al. 2006; see also Chap. 16, Malusà 2018).

2.11.3 Standard Glasses

The standard glasses used for neutron dosimetry are produced with uniform uranium concentrations so that as a result of irradiation, their corresponding muscovite detectors receive a uniform-induced track density, usually over a large area of about 1 cm^2. The tracks in each muscovite detector should be counted on a regular pattern covering the whole available area using the same counting criteria as with counting N_s on the grain surfaces. The simplest method is to move around the muscovite on a regular 1 or 0.5 mm grid and at each location, count the tracks in a predetermined area of the graticule. The number of locations and the number of grid squares counted at each will depend on the track density. Typically tracks are counted at a number of locations to give a total track count of at least 1000. It is good practice to count each glass over different areas at least twice to verify the track density obtained and to increase the precision on the combined measurement. The track density (per cm^2) is determined from the total number of tracks and the total area counted. If a significant and reproducible difference is found in standard glass track density along the irradiation canister, then this indicates a neutron flux gradient and an intermediate value should be interpolated for each mount in the package. Calculation of the uranium concentration for individual mineral grains may be estimated approximately by measuring the ratio of the induced track density over the grain to the induced track density in an external detector over the standard glass multiplied by the known uranium content of the standard glass.

2.11.4 Automation of the EDM

To determine the ratio of spontaneous to induced tracks, identical areas are counted on each mineral grain and its muscovite detector mirror image. A typically used sequence of steps is to select a suitable grain, count the spontaneous tracks, locate its mirror image on the muscovite and count the induced tracks. Before counting an external detector mount, it is recommended to scan the muscovite at low power to check that the detector had remained in close contact with the mount during irradiation. Grains with good contact and sufficient uranium and N_i will have sharp, clearly defined mirror images and grain boundaries in the muscovite. Areas of poor contact, indicated by diffuse, rounded grain image boundaries often with a splayed track pattern should be avoided, as they will give an underestimate for the induced track density.

The ability to select suitable grains for counting only comes after the completion of a significant amount of training to recognise identifiable features associated with each grain. Suitable grains include those having well-etched tracks, sharp polishing scratches, reasonably uniform track density and minimum interference from inclusions, cracks and dislocations. Where spontaneous track densities (N_s) are low, the numbers of tracks in each grain, and the apparent single-grain ages, can vary substantially due to the natural statistical variation of the decay process. It is easy to select only those grains with relatively higher track densities, but this can lead to a seriously biased age. In such cases, it is important to ensure that grains are selected covering the whole range of variation in track densities, even including grains with no tracks if they are present. Having selected a suitable grain, the spontaneous tracks are counted, but the zone within the range of one track of any external grain margin should be avoided.

Locating the corresponding area on the muscovite can be carried out manually, although this is extremely tedious and mistakes are easily made resulting in erroneous ages. However, the time-consuming task of locating matching points on the grain mount and its external detector is now mostly automated using a computer-controlled microscope stage system (e.g. Smith and Leigh-Jones 1985).

Such automated stage systems are now almost universally used for the EDM and provide a much faster and more reliable technique for accurately and repeatedly locating matching points on a muscovite external detector. Another advantage of such automated methods is that they provide a framework for the systematic collection and organisation of the FT data.

An example of the sequence followed using an automated stage system involves the following steps:

- Find and mark the zero reference point (e.g. the copper disc in Fig. 2.2).
- Coarse alignment of the mount and detector using at least two different pinprick positions (alignment marks) preferably between opposite corners of the mount.
- Refine the alignment using mineral grains and their induced track images.
- Select and label suitable grains for counting.
- Count spontaneous and induced tracks over each grain.
- Measure confined track lengths as these are observed.
- Measure Dpars (see Sect. 2.11.7) for each grain from which age or length data are collected—using only etch pits from spontaneous tracks.
- Save all data to a computer file.

Most systems are capable of operating in three axes, so that relative offsets in x, y and z, as well as rotations of the muscovite relative to the mount can be corrected for by automated movements of the stage. Once the alignment procedure is completed, the stage system retains an exact knowledge of the positions of matching points on the mineral mount and their mirror image positions on the muscovite, and can move between them as required.

2.11.5 FT Length Measurements

In order to carry out thermal history modelling of a sample measurement of the distribution of horizontal or close-to-horizontal confined FT lengths (i.e. below the polished surface within the mineral) is a critical parameter required to accompany any FT age (Gleadow et al. 1986). A variety of measurements have been used in FT dating studies to estimate the distribution of track lengths (e.g. Bhandari et al. 1971; Wagner and Storzer 1972; Dakowski 1978). Some of these measurements (e.g. projected lengths) contain little useful information about the true length distribution (Dakowski 1978; Green 1981; Laslett et al. 1982). A much better procedure is to measure the lengths of *confined* tracks that do not intersect the surface and are entirely located within the crystal interior but have been etched from an intersection with either a track at the surface or a crack or cleavage plane emerging at the surface (see Chap. 1, Hurford 2018). These tracks are called TINTs (track-in-track) and TINCLEs (track-in-cleavage) after Lal et al. (1969), who first suggested their use. However, the measurement of TINCLE fission tracks may lead to unreliable data, so they should be avoided (e.g. Donelick et al. 2005). The measurement of semi-tracks (the preserved parts of tracks that have intersected a polished prismatic surface, i.e. the spontaneous tracks counted for age determination) is a further

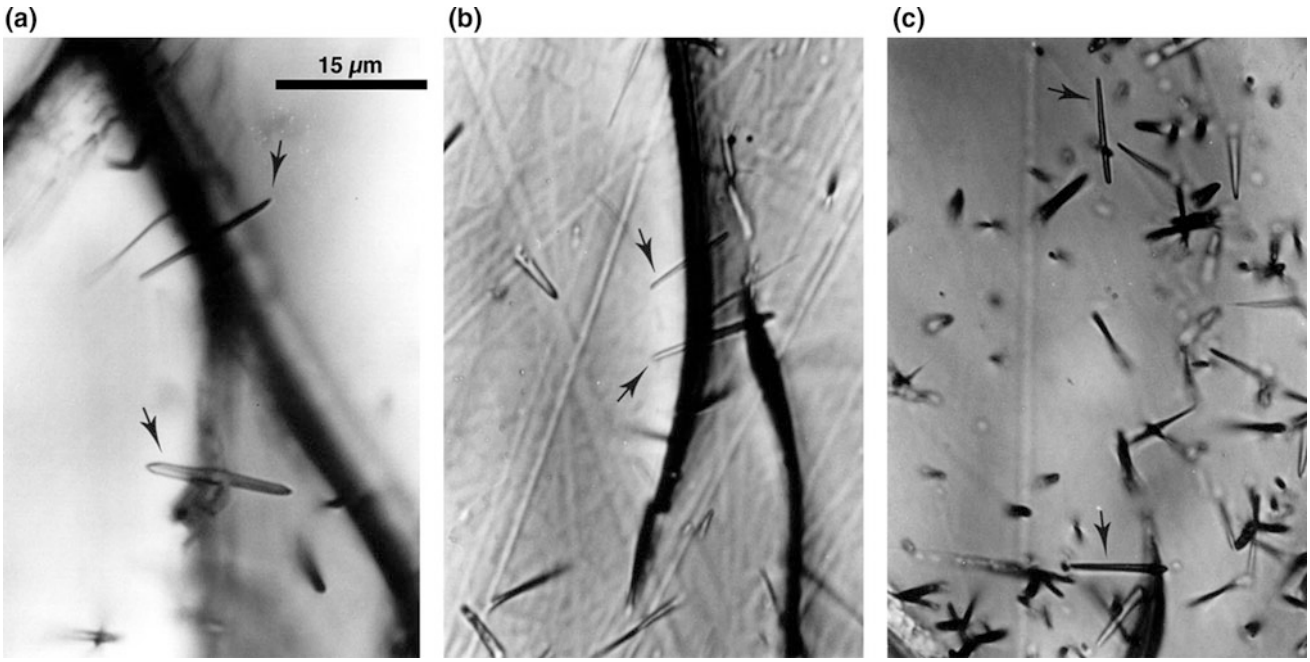

Fig. 2.6 Confined spontaneous fission tracks in apatite suitable for length measurements. TINCLEs are indicated by arrows in frames **(a)** and **(b)**, while frame **(c)** shows one TINT (top) and one TINCLE (bottom). Scale is similar for each frame

possibility (Laslett and Galbraith 1996) that may have some advantages in automated measurement systems (see also Chap. 4, Gleadow et al. 2018). For further information on the measurement of FT lengths in apatite see Gleadow et al. (2002) and Donelick et al. (2005), and zircon see Tagami (2005).

Only tracks with rounded or angular ends should be measured, indicating that the etchant has penetrated right to the end of the track to reveal its full length. Prior to measurement of confined tracks, care should be taken that the mount is clean and dry, as liquids, especially oils from greasy fingerprints, can lodge in the end of a confined track making the tip of the track very difficult to see. Washing the mount in a strong detergent will usually remove any liquid from the confined tracks. Examples of well-etched confined tracks in apatite are shown in Fig. 2.6.

In principle, it is possible to measure both the horizontal and vertical components of the length of confined tracks to give their actual length, regardless of their orientation. In practice on most of the older microscopes however, the vertical distance is not easily measured and reduces the precision of the overall measurement. A simpler and more rigorous procedure is to select only those confined tracks, which are ±10 °C from the horizontal (Ketcham et al. 2009) and to measure their apparent length directly. Such measurements have the closest relationship to the true length distribution and are less subject to inherent sampling bias than other parameters (Laslett et al. 1982). Horizontal tracks can be readily identified as those that are in focus along their entire length under a high-power objective. In reflected light, horizontal tracks are very obvious because they have a very bright reflection, without the diffraction bands, which characterise shallowly dipping tracks. Scanning in reflected light (if available) for suitable horizontal confined tracks for measurement can be very useful. In many cases, though certainly not all, horizontal tracks can show up very obviously because they have a bright reflection without the diffraction bands, which often characterise shallow dipping tracks.

Most laboratories carry out confined track length measurements using a drawing tube attachment to a microscope in association with a digitising tablet attached to a computer. The drawing tube superimposes an image of the digitising tablet with its cursor on the usual microscope image. The cursor carries a bright light-emitting diode to mark the measuring point in the optical image. Once a suitable track is located the cursor is simply moved to each end of the image of the track in turn and the positions marked. The raw coordinates for the track ends are translated into a length measurement, and these data are transferred to a computer for storage and statistical analysis. For each length measured, the azimuth direction of the *c*-axis from the elongation of the track etch pit is usually carried out at the same time as a reference frame for the orientation of the confined tracks. The sample mount should be scanned systematically and the lengths of the confined tracks measured.

Most of the time during a track length analysis is spent locating suitable tracks. In terms of the minimum number of lengths that should be counted, there is no firm rule of thumb, but one should endeavour to collect as much length data as possible. However, samples containing both long and short tracks, which usually reflect a more complicated thermal history, should require more measurements. Mean track length values in apatites generally stabilise after ~50–120 measurements (Barbarand et al. 2003a). However, using *c*-axis projection to normalise track lengths in relation to crystallographic angle due to differences in annealing characteristics with orientation leads to improved measurement reproducibility and earlier stabilisation of a mean length value compared to non-projected tracks (Ketcham et al. 2007). In detrital zircons, length measurements are not carried out routinely due to complications arising from the variability in etching requirements often encountered between grains, possibly arising from the presence of different provenance populations, but mainly due to variations in α-radiation damage (Bernet and Garver 2005). In detrital apatites, it is important to measure confined track lengths only in those crystals that are dated, so that discrete grain-age populations can be identified and robust geological interpretations made. Several methods for decomposing FT ages using peak fitting programs are available (e.g. Brandon 1992; Galbraith and Laslett 1993; Vermeesch 2009; see also Chap. 6, Vermeesch 2018).

2.11.6 Californium (^{252}Cf) Irradiation

^{252}Cf irradiation is a technique used to enhance the number of measurable confined lengths in apatite (Donelick and Miller 1991) and also to lessen observer bias (Ketcham 2005). Such irradiations, carried out prior to chemical etching, may be performed on a masked area of the grain mount or on a second grain mount prepared for each sample. Alternatively, one could use the same mount made for N_s determination and re-etch for length measurements after counting for N_s (see Donelick et al. 2005). By placing grain mounts under vacuum at a distance of several mm from a planar ^{252}Cf spontaneous fission fragment source ($T_{1/2}$ = 2.645 yr), a substantial number of fission particles are created, which penetrate the exposed internal grain surface. The resultant tracks act as 'pathways' for the etchant to reach confined tracks at depth below the exposed grain surface within the apatite, effectively increasing the number of confined FT lengths available for measurement (see Donelick et al. 2005). This method has been widely applied to samples with low uranium concentration and/or those young in age where insufficient track-in-tracks (TINTs) were observed. In zircon, which is a denser mineral, ^{252}Cf irradiation does not work well for implanting long tracks and other techniques for increasing the number of measurable confined tracks, such as irradiation by heavy nuclides and artificial fracturing have been reviewed by Yamada et al. (1998).

2.11.7 Kinetic Parameters

FT annealing in apatite is a complicated, nonlinear process that is not completely understood, but is known to be dominantly controlled by temperature (markedly so above >60 °C), the duration of heating and to a lesser degree by crystallographic orientation (e.g. Donelick et al. 2005). However, annealing is also related to a complex interplay of anion (Cl, F, OH) and cation substitutions (e.g. REE, Mn, Sr, Fe, Si), with Cl playing a primary role (Green et al. 1985). REE in more F-rich apatites have been suggested to exercise some control on annealing (Barbarand et al. 2003b) as have some other possible chemical factors as outlined by Donelick et al. (2005) and Spiegel et al. (2007). The bulk track-etching rate of apatite has also been proposed as a proxy for bulk chemical composition, and this involves measurement of the Dpar—the arithmetic mean of FT etch pit lengths measured parallel to the crystallographic *c*-axis (e.g. Donelick 1993; Burtner et al. 1994).

Dpar length and Cl content are the two kinetic parameters most routinely measured and should be collected from every grain analysed for either age or track length data. Along with FT age and length data, the measurement of either parameter is considered essential for carrying out quantitative thermal history modelling of individual apatite grains or populations of grains. Thermal history models in common use can accommodate the input of either parameter. The choice of which measurement should be preferred, however, is still the subject of some debate (e.g. Barbarand et al. 2003b; Green et al. 2005; Hurford et al. 2005; Donelick et al. 2005).

Data for both parameters (as for age and length data) should only be acquired on prismatic sections parallel to the crystallographic *c*-axis, and this orientation can be readily checked by the presence of sharp polishing scratches and the alignment of etch pit openings under reflected light parallel to the *c*-axis (see Donelick et al. 2005).

The measurement of Dpar for a conventional microscope set-up is essentially the same as for track length measurement, but in this case the scale of measurement is considerably smaller. With digital imaging (see Sect. 2.12 and Chap 4, Gleadow et al. 2018) Dpars, however, can now be measured automatically with greater resolution down to almost the pixel level, within a matter of seconds and the smaller parameter Dper (the etch pit minor axis perpendicular to the *c*-axis) can also be resolved, allowing for a more precise and complete characterisation of etch pit geometry.

Measurement of apatite Cl content has now largely become a routine procedure. However, traditionally it involves another analytical step and is perceived as being more expensive and time-consuming, in that grain *x*–*y* coordinates recorded from the measurement of both grain ages and track lengths are now required to be transferred to a suitable stage for electron probe microanalysis for grain-by-grain halogen analysis (F and Cl content). Special care should be taken when carrying out such analysis on apatite as the halogen X-ray intensity can fluctuate strongly with operating conditions, grain orientation and bulk F and Cl content (Goldoff et al. 2012; Stock et al. 2015). The use of infrared microspectroscopy for the semi-quantitative determination of apatite anion composition has been described by Siddall and Hurford (1998), but is not used routinely. The measurement of Cl content in apatite using LA-ICP-MS (Chew et al. 2014) is an important development towards collecting kinetic information together with uranium (and REE) content for a more integrated approach towards data acquisition for FT analysis.

2.12 Digital Imaging and Automated FT Analysis

Conventional FT counting is very labour-intensive. However, new analytical approaches are now promising significant improvements in data quality and analytical productivity in FT analysis. Gleadow et al. (2009, 2015) described a method that combines autonomous digital microscopy and automatic image analysis for the recognition and counting of fission tracks in minerals such as apatite, along with new tools for the enhanced measurement of Dpar and FT lengths. This new technique takes full advantage of the capabilities of the new generation of digital microscopes, such as the Zeiss Axio-Imager series. Much of the operator time previously tied to the microscope is now freed up to do other things as the microscope/software system captures and processes the images autonomously, without the need for operator involvement after the first setting up has been completed. Multiple slides can be imaged overnight, and the processed images analysed offline on a computer using the analysis software. Digital coordinates of analysed grains are exported to other computer-operated devices such as a laser ablation stage or an electron probe microanalyser stage, for further analysis. This new approach is described in more detail in Chap. 4, (Gleadow et al. 2018).

Acknowledgements We are grateful to numerous past and present researchers and graduate students in the Thermochronology Group at the University of Melbourne for their contributions towards establishing some of the methodologies described in this work. The National Collaborative Research Infrastructure Strategy AuScope programme supports the University of Melbourne thermochronology facility. Martin Danišík and Paul O'Sullivan provided thoughtful and constructive reviews, which helped to improve the clarity of this work.

References

Arne DC, Green PF, Duddy IR, Gleadow AJW, Lambert IB, Lovering JF (1989) Regional thermal history of the Lennard Shelf, Canning Basin, from apatite fission track analysis: Implications for the formation of Pb-Zn deposits. Aust J Earth Sci 36:495–513

Barbarand J, Carter A, Hurford T (2003a) Variation in apatite fission-track length measurement: implications for thermal history modelling. Chem Geol 198:77–106

Barbarand J, Carter A, Wood I, Hurford T (2003b) Compositional and structural control of fission-track annealing in apatite. Chem Geol 198:107–137

Bellemans F, De Corte F, Van den Haute P (1995) Composition of SRM and CN U-doped glasses: significance for their use as thermal neutron monitors in fission track dating. Radiat Meas 24:153–160

Bernet M, Garver JI (2005) Fission-track analysis of detrital zircon. In: Reiners P, Ehlers T (eds) Low-temperature thermochronology. Rev Min Geochem 58:205–238

Bhandari N, Bhat SC, Lal D, Rajagoplan G, Tamhane AS, Venkatavaradan VS (1971) Fission fragment tracks in apatite: recordable track lengths. Earth Planet Sci Lett 13:191–199

Brandon MT (1992) Decomposition of fission-track grain-age distributions. Am J Sci 292:535–564

Braun J, van der Beek P, Batt G (2006) Quantitative thermochronology. Cambridge University Press, Cambridge

Burtner RL, Nigrini A, Donelick RA (1994) Thermochronology of Lower Cretaceous source rocks in the Idaho-Wyoming Thrust Belt. Bull Am Assoc Petrol Geol 78:1613–1636

Calk LC, Naeser CW (1973) The thermal effect of a basalt intrusion on fission tracks in quartz monzonite. J Geol 81:189–198

Callahan J (1987) A nontoxic heavy liquid and inexpensive filters for separation of mineral grains. J Sed Pet 57:765–766

Carlson WD, Donelick RA, Ketcham RA (1999) Variability of apatite fission-track annealing kinetics: I. Experimental results. Am Min 84:1213–1223

Carpenter SB, Reimer GM (1974) Standard reference materials: calibrated glass standards for fission track use. Nat Bur Stand Spec Pub 260–49

Carrapa B, DeCelles PG, Reiners PW, Gehrels GE, Sudo M (2009) Apatite triple dating and white mica $^{40}Ar/^{39}Ar$ thermochronology of syntectonic detritus in the Central Andes: a multiphase tectonothermal history. Geology 37:407–410

Carter A, Moss SJ (1999) Combined detrital-zircon fission-track and U-Pb dating: a new approach to understanding hinterland evolution. Geology 27:235–238

Chew DM, Donelick RA (2012) Combined apatite fission track and U–Pb dating by LA-ICP-MS and its application in apatite provenance analysis. In: Sylvester P (ed) Quantitative mineralogy and microanalysis of sediments and sedimentary rocks. Mineralogical Association of Canada Short Course, pp 219–248

Chew DM, Donelick RA, Donelick MB, Kamber B, Stock MJ (2014) Apatite chlorine concentration measurements by LA-ICP-MS. Geostand Geoanalyt Res 38:23–35

Chew DM, Babechuk MG, Cogné N, Mark C, O'Sullivan GJ, Henrichs IA, Doepke D, Mckenna CA (2016) (LA, Q)-ICPMS trace-element analyses of Durango and McClure Mountain apatite and implications for making natural LA-ICPMS mineral standards. Chem Geol 435:35–48

Chisholm E-K, Sircombe K, DiBugnara D (2014) Handbook of geochronology mineral separation laboratory techniques. Geoscience Australia Record 2014/46, 45 p

Coutand I, Carrapa B, Deeken A, Schmitt AK, Sobel ER, Strecker MR (2006) Propagation of orographic barriers along an active range front: insights from sandstone petrography and detrital apatite fission-track thermochronology in the intramontane Angastaco basin, NW Argentina. Basin Research 18:1–26

Cox R, Košler J, Sylvester P, Hodych J (2000) Apatite fission-track (FT) dating by LAM-ICO-MS analysis. Abstracts Goldschmidt 2000. J Conf Abstracts 5(2):322

Dakowski M (1978) Length distributions of fission tracks in thick crystals. Nucl Track Detect 28:181–189

Danišík M, Pfaff K, Evans N, Manoloukos C et al (2010) Tectonothermal history of the Schwarzwald Ore District (Germany): an apatite triple dating approach. Chem Geol 278:58–69

Danišík M (2018) Integration of fission-track thermochronology with other geo-chronologic methods on single crystals (Chapter 5). In: Malusà MG, Fitzgerald PG (eds) Fission-track thermochronology and its application to geology. Springer, Berlin

De Corte F, Bellemans F, van den Haute P, Inglebrecht C, Nicholl C (1998) A new U doped glass certified by the European Commission for calibration of fission-track dating. In: den Haute Van, De Corte F (eds) Advances in fission-track geochronology. Springer, Dordrecht, pp 67–78

Dias ANC, Chemale F Jr, Soares CJ, Guedes S (2017) A new approach for electron microprobe zircon fission track thermochronology. Chem Geol 459:129–136

Donelick R (1993) Apatite etching characteristics versus chemical composition. Nucl Tracks Radiat Meas 21:604

Donelick RA, Miller DS (1991) Enhanced TINT fission track densities in low spontaneous track density apatites using ^{252}Cf-derived fission fragments tracks: a model and experimental observations. Nucl Tracks Radiat Meas 18:301–307

Donelick RA, O'Sullivan PB, Ketcham RA (2005) Apatite fission-track analysis. In: Reiners P, Ehlers T (eds) Low-temperature thermochronology. Rev Min Geochem 58:49–94

Dumitru TA (2000) Fission-track geochronology. In: Noller JS, Sowers JM, Lettis, WR (eds) Quaternary geochronology: methods and applications. Am Geophys Union Ref Shelf 4, Washington, DC, American Geophysical Union, pp 131–155

Enkelmann E, Jonckheere R, Wauschkuhn B (2005) Independent fission-track ages (ϕ-ages) of proposed and accepted apatite age standards and a comparison of ϕ-, Z-, ζ- and ζ0-ages: implications for method calibration. Chem Geol 222:232–248

Evans NJ, McInnes BIA, McDonald B, Danišík M, Becker T, Vermeesch P, Shelley M, Marillo-Sialer E, Patterson DB (2015) An in situ technique for (U–Th–Sm)/He and U-Pb double dating. J Anal At Spectrom 30:1636–1645

Fleischer RL, Price PB (1964) Techniques for geological dating of minerals by chemical etching of fission fragment tracks. Geochim et Cosmochim Acta 28:1705–1714

Fleischer RL, Price PB, Walker RL (1975) Nuclear tracks in solids: principles and applications. University of California Press, Berkeley

Galbraith RF (2005) Statistics for fission track analysis. Chapman & Hall, Boca Raton

Galbraith RF, Laslett GM (1993) Statistical models for mixed fission-track ages. Nucl Track Radiat Meas 21:459–470

Gallagher K, Brown R, Johnson C (1998) Fission track analysis and its applications to geological problems. Ann Rev Earth Planet Sci 26:519–572

Garver JI (2003) Etching age standards for fission track analysis. Radiat Meas 37:47–54

Garver JI, Brandon MT, Roden-Tice MK, Kamp PJJ (1999) Exhumation history of orogenic highlands determined by detrital fission track thermochronology. In: Ring U, Brandon MT, Willett SD, Lister GS (eds) Exhumation processes: normal faulting, ductile flow, and erosion. Geol Soc London Spec Pub 154:283–304

Giese J, Seward D, Stuart FM, Wüthrich E et al (2009) Electrodynamic disaggregation: does it affect apatite fission-track and (U-Th)/He analyses? Geostand Geoanal Res 34:39–48

Gleadow AJW (1978) Anisotropic and variable track etching characteristics in natural sphenes. Nuclear Track Detect 2:105–117

Gleadow AJW (1981) Fission track dating methods: what are the real alternatives. Nucl Tracks 5:3–14

Gleadow AJW (1984) Fission track dating methods—II: a manual of principles and techniques. Workshop on fission track analysis: principles and applications. James Cook University, Townsville, Australia, 4–6 September 1984, 35 p

Gleadow AJW, Lovering JF (1974) The effect of weathering on fission track dating. Earth Planet Sci Letts 22:163–168

Gleadow AJW, Lovering JF (1978) Thermal history of granitic rocks from Western Victoria: a fission-track study. J Geol Soc Aust 25:323–340

Gleadow AJW, Hurford AJ, Quaife RD (1976) Fission track dating of zircon: improved etching techniques. Earth Planet Sci Letts 33:273–276

Gleadow AJW, Duddy IR, Green PF, Lovering JF (1986) Confined fission track lengths in apatite: a diagnostic tool for thermal history analysis. Contrib Mineral Petrol 94:405–415

Gleadow AJW, Belton DX, Kohn BP, Brown RW (2002) Fission track dating of phosphate minerals and the thermochronology of apatite. Rev Min Geochem 48:579–630

Gleadow AJW, Gleadow SJ, Belton DX, Kohn BP, Krochmal MS (2009) Coincidence mapping a key strategy for automated counting in fission track dating. In: Ventura B, Lisker F, Glasmacher UA (eds) Thermochronological methods: from palaeotemperature constraints to landscape evolution models. Geol Soc Lond Spec Pub 324, pp 25–36

Gleadow A, Harrison M, Kohn B, Lugo-Zazueta R, Phillips D (2015) The Fish Canyon Tuff: a new look at an old low-temperature thermochronology standard. Earth Planet Sci Letts 424:95–108

Gleadow A, Kohn B, Seiler C (2018) The future of fission-track thermochronology (Chapter 4). In: Malusà MG, Fitzgerald PG (eds) Fission-track thermochronology and its application to geology. Springer, Berlin

Goldoff B, Webster JD, Harlov DE (2012) Characterization of fluor-chloroapatites by electron microprobe analysis with a focus on time-dependent intensity variation of halogens. Am Min 97:1103–1115

Gombosi DJ, Garver JI, Baldwin SL (2014) On the development of electron microprobe zircon fission-track geochronology. Chem Geol 363:312–321

Green PF (1981) "Track-in-track" length measurements in annealed apatites. Nucl Tracks 5:121–128

Green PF, Hurford AJ (1984) Neutron dosimetry in fission track dating: a theoretical background and some practical precautions. Nucl Tracks 9:231–241

Green PF, Duddy IR, Gleadow AJW, Tingate PR, Laslett GM (1985) Fission track annealing in apatite: track length measurements and the form of the Arrhenius plot. Nucl Tracks 10:323–328

Green PF, Duddy IR, Hegarty KA (2005) Comment on "Compositional and structural control of fission track annealing in apatite" by Barbarand J, Carter A, Wood I and Hurford AJ, Chem Geol 198 (2003);107–137; Chem Geol 214:351–358

Haack UH, Gramse M (1972) Survey of garnets for fossil fission tracks. Contrib Mineral Petrol 34:258–260

Hasebe N, Barbarand J, Jarvis K, Carter A, Hurford AJ (2004) Apatite fission-track chronometry using laser ablation ICP-MS. Chem Geol 207:135–145

Hasebe N, Carter A, Hurford AJ, Arai S (2009) The effect of chemical etching on LA-ICP-MS analysis in determining uranium concentration for fission-track chronometry. In: Ventura B, Lisker F, Glasmacher UA (eds) Thermochronological methods: from palaeotemperature constraints to landscape evolution models. Geol Soc Lond Spec Pub 324, pp 37–46

Hasebe N, Tamura A, Arai S (2013) Zeta equivalent fission-track dating using LA-ICP-MS and examples with simultaneous U-Pb dating. Island Arc 22:280–291

Hejl E (1998) The Zeta-Potential of apatite and zircon: its significance for mineral separation. On Track—Newsletter of the International Fission Track Community 8(no 1, Issue 16):7–8

http://zeiss-campus.magnet.fsu.edu/articles/basics/kohler.html. Zeiss resource—Configuring a Microscope for Köhler Illumination In: Education in microscopy and digital imaging. Accessed 5 July 2016

Hurford AJ (1990) Standardization of fission track dating calibration: recommendation by the fission track working group of the I.U.G.S. subcommission on geochronology. Chem Geol (Isot Geosci Sect) 80:171–178

Hurford AJ (1998) Zeta: the ultimate solution to fission-track analysis calibration or just an interim measure? In: van den Haute P, De Corte F (eds) Advances in fission-track geochronology. Kluwer Academic Publishers, Dordrecht, pp 19–32

Hurford AJ (2018) An historical perspective on fission-track thermochronology (Chapter 1) In: Malusà MG, Fitzgerald PG (eds) Fission-track thermochronology and its application to geology. Springer, Berlin

Hurford AJ, Green PF (1982) A user's guide to fission track dating calibration. Earth Planet Sci Lett 59:343–354

Hurford AJ, Green PF (1983) The zeta age calibration of fission-track dating. Chem Geol Isot Geosci 1:285–317

Hurford AJ, Barbarand J, Carter A (2005) Reply to comment on "Compositional and structural control of fission track annealing in apatite" by Barbarand J, Carter A, Wood I, Hurford AJ, Chem Geol 198(2003):107–137; Chem Geol 214:359–361

Ijlst L (1973) New diluents in heavy liquid mineral separation and an improved method for the recovery of liquids. Am Min 58:1084–1087

Ito K, Hasebe N (2011) Fission-track dating of Quaternary volcanic glass by stepwise etching. Radiat Meas 46:76–182

Iwano H, Danhara T (1998) A re-investigation of the geometry factors for fission-track dating of apatite, sphene and zircon. In: van den Haute P, De Corte F (eds) Advances in fission-track geochronology. Kluwer Academic Publishers, Dordrecht, pp 47–66

Jonckheere R, Ratschbacher L, Wagner GA (2003) A repositioning technique for counting induced fission tracks in muscovite external detectors in single-grain dating of minerals with low and inhomogeneous uranium concentrations. Radiat Meas 37:217–219

Ketcham RA (2005) Forward and inverse modeling of low-temperature thermochronometry data. In: Reiners P, Ehlers T (eds) Low-temperature thermochronology. Rev Mineral Geochem 58:275–314

Ketcham RA, Carter A, Donelick RA, Barbarand J, Hurford AJ (2007) Improved measurement of fission-track annealing in apatite using c-axis projection. Am Min 92:789–798

Ketcham RA, Donelick RA, Balestrieri ML, Zattin M (2009) Reproducibility of apatite fission-track length data and thermal history reconstruction. Earth Planet Sci Letts 284:504–515

Kohn BP, Gleadow AJW, Brown RW, Gallagher K, Lorencak M, Noble WP (2005) Visualising thermotectonic and denudation histories using apatite fission track thermochronology. In: Reiners P, Ehlers T (eds) Low-temperature thermochronology, Rev Min Geochem 58:527–565

Košler M, Svojtka M (2003) Present trends and the future of zircon in geochronology: laser ablation ICPMS. In: Manchar JM, Hoslin PWO (eds) Zircon. Rev Min Geochem 54:243–275

Krishnaswami S, Lal D, Prabhu N, MacDougall D (1974) Characteristics of fission tracks in zircon: applications to geochronology and cosmology. Earth Planet Sci Letts 22:51–59

Lal D, Rajan RS, Tamhane AS (1969) Chemical composition of nuclei of $Z > 22$ in cosmic rays using meteoritic minerals as detectors. Nature 221:33–37

Laslett GM, Galbraith RF (1996) Statistical properties of semi-tracks in fission track analysis. Radiat Meas 26:565–576

Laslett GM, Kendall WS, Gleadow AJWLaslett GM, Kendall WS, Gleadow AJW, Duddy IR (1982) Bias in measurement of fission-track length distributions. Nucl Tracks 6:79–85

Lisker F, Ventura B, Glasmacher UA (2009) Apatite thermochronology in modern geology. In: Ventura B, Lisker F, Glasmacher UA (eds) Thermochronological methods: from palaeotemperature constraints to landscape evolution models. Geol Soc Lond Spec Publ 324, pp 1–23

Malusà MG (2018) A guide for interpreting complex detrital age patterns in stratigraphic sequences (Chapter 16). In: Malusà MG, Fitzgerald PG (eds) Fission-track thermochronology and its application to geology. Springer, Berlin

Malusà MG, Garzanti E (2018) The sedimentology of detrital thermochronology (Chapter 7). In: Malusà MG, Fitzgerald PG (eds) Fission-track thermochronology and its application to geology. Springer, Berlin

Montario MJ, Garver JI (2009) The thermal evolution of the Grenville terrane revealed through U-Pb and fission-track analysis of detrital zircon from Cambro-Ordovician quartz arenites of the Potsdam and Galway formations. J Geol 117:595–614

Naeser CW (1976) Fission track dating. US Geological Survey Open-File Report 76-190 86 p

Naeser CW, Dodge FCW (1969) Fission track ages of accessory minerals from granitic rocks of the Central Sierra Nevada batholith, California. Geol Soc Am Bull 80:2201–2212

Naeser CW, McKee EH (1970) Fission-track and K-Ar ages of Tertiary ash-flow tuffs, north central Nevada. Geol Soc Am Bull 81:3375–3384

Naeser ND, Zeitler PK, Naeser CW, Cerveny PF (1987) Provenance studies by fission track dating of zircon—etching and counting procedures. Nucl Tracks Radiat Meas 13:121–126

Naeser CW, Naeser ND, Newell WL, Southworth S, Edwards LE, Weems RE (2016) Erosional and depositional history of the Atlantic passive margin as recorded in detrital zircon fission-track ages and lithic detritus in Atlantic coastal plain sediments. Am J Sci 316:110–168

Ravenhurst CE, Donelick RA (1992) Fission track thermochronology. In: Zentilli M, Reynolds PM (eds) Short course handbook on low temperature thermochronology. Mineral Assoc Can, Ottawa, pp 21–42

Reiners PW, Thomson SN, McPhilips D, Donelick RA, Roering JJ (2007) Wildfire thermochronology and the fate and transport of apatite in hillslope and fluvial environments. J Geophy Res 112: F04001. https://doi.org/10.1029/2007jf000759

Seward D, Spikings R, Viola G, Kounov A, Ruiz GMH, Naeser N (2000) Etch times and operator variation for spontaneous track length measurements in apatites: an intra-laboratory check. OnTrack 10(21):16–21

Siddall R, Hurford AJ (1998) Semi-quantitative determination of apatite anion composition for fission-track analysis using infrared microspectroscopy. Chem Geol 150:181–190

Smith MJ, Leigh-Jones P (1985) An automated microscope scanning stage for fission-track dating. Nucl Tracks 10:395–400

Soares C, Guedes S, Hadler J, Mertz-Kraus R, Zack T, Iunes P (2014) Novel calibration for LA-ICP-MS-based fission-track thermochronology. Phys Chem Miner 41:65–73

Sobel ER, Seward D (2010) Influence of etching conditions on apatite fission-track etch pit diameter. Chem Geol 271:59–69

Sperner B, Jonckheere R, Pfander J (2014) Testing the influence of high-voltage mineral liberation on grain size, shape and yield and on fission track and $^{40}Ar/^{39}Ar$ dating. Chem Geol 371:83–95

Spiegel C, Kohn BP, Raza A, Rainer T, Gleadow AJW (2007) The effect of long-term low temperature exposure on apatite fission track stability: A natural annealing experiment in the deep ocean. Geochim Cosmochim Acta 71:4512–4537

Stock MJ, Humphreys MCS, Smith VC, Johnson RD et al (2015) New constraints on electron-beam induced halogen migration in apatite. Am Min 100:281–293

Tagami T (1987) Determination of zeta calibration constant for fission track dating. Nucl Tracks Radiat Meas 13:127–130

Tagami T (2005) Zircon fission-track thermochronology and applications to fault studies. In: Reiners P, Ehlers T (eds) Low-temperature thermochronology. Rev Min Geochem 58:95–122

Tagami T, O'Sullivan PB (2005) Fundamentals of fission-track thermochronology. In: Reiners P, Ehlers T (eds) Low-temperature thermochronology. Rev Min Geochem 58:19–47

Torresan M (1987) The use of sodium polytungstate in heavy mineral separations. US Geological Survey of Open-File Report 87-590, 18 p

van den Haute P, De Corte F, Jonckheere R, Bellemans F (1998) The parameters that govern the accuracy of fission-track age determinations: a-reappraisal. In: van den Haute P, De Corte F (eds) Advances in fission-track geochronology. Kluwer Academic Publishers, Dordrecht, pp 33–46

Vermeesch P (2009) Radialplotter: a java application for fission track, luminescence and other radial plots. Radiat Meas 44:409–410

Vermeesch P (2017) Statistics for LA-ICP-MS based fission track dating. Chem Geol 456:19–27

Vermeesch P (2018) Statistics for fission-track thermochronology (Chapter 6). In: Malusà MG, Fitzgerald PG (eds) Fission-track thermochronology and its application to geology. Springer, Berlin

Wagner GA, Storzer D (1972) Fission track length reductions in minerals and the thermal history of rocks. Trans Amer Nucl Soc 15:127–128

Wagner GA, van den Haute P (1992) Fission track dating. Kluwer Academic, Dordrecht

Yamada R, Yoshioka T, Watanabe K, Tagami T, Nakamura H, Hashimoto T, Nishimura S (1998) Comparison of experimental techniques to increase the number of measurable confined fission tracks in zircon. Chem Geol (Isotope Geosci Sect) 149:99–107

Zaun PE, Wagner GA (1985) Fission-track stability in zircons under geological conditions. Nucl Tracks 10:303–307